Hochschule
München (HM)
University of
Applied Sciences

Laboratory for
Mechatronic
and Renewable
Energy Systems
(LMRES)

Artificial neural networks in electrical drive systems

LMRES team and Christoph M. Hackl
christoph.hackl@hm.edu

24.09.2025 – KI-Power Symposium, Nuremberg

Outline

Outline

Outline

Introduction: LMRES

Research environment: HM (www.hm.edu), ISES (ises.hm.edu) and LMRES (lmres.ee.hm.edu)

HM – Munich University of Applied Sciences

- 14 departmens
- >18.000 students
- ~480 professors
- 3 campuses

ISES – Institute for Sustainable Energy Systems

- 8 research labs (8 professors)
- 39 PhD candidates

LMRES – Laboratory for Mechatronic and Renewable Energy Systems

- International team
- 15 PhD candidates (status 2025)
- >150 publications / >9.2 Mio. € raised

Introduction: LMRES

Research projects and research goals

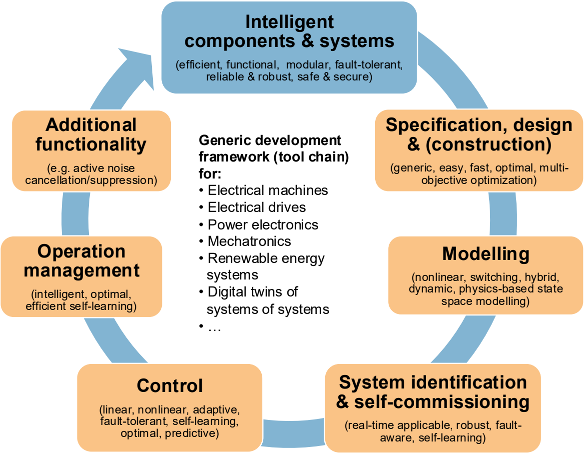

Introduction: LMRES

Interdisciplinary expertise & publications (for more details see https://lmres.ee.hm.edu)

System identification [9–26]

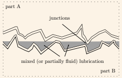

Friction [27–29]

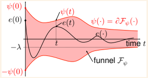

Non-identifier based adaptive control [14, 27, 30–46]

Paper coating machines [4–8]

Supervision & teaching (Award) [159–165]

Mechatronics & robotics [27, 28, 40, 46–58]

Mechatronic and renewable energy systems

Electro-active polymers [1–3]

Power electronics [19–21, 46, 58–88]

Wind energy, renewables & smart grid [13–15, 44, 46, 57, 58, 60, 61, 67, 68, 70–72, 74, 79, 85, 93–95, 98, 100, 107, 112, 120, 132, 136, 141–158]

Electrical machines & drives [13, 15, 17, 23–27, 30, 32, 33, 45, 46, 51, 55, 57, 69, 77, 78, 80, 89–140]

Introduction: LMRES

Used hardware setups (selection)

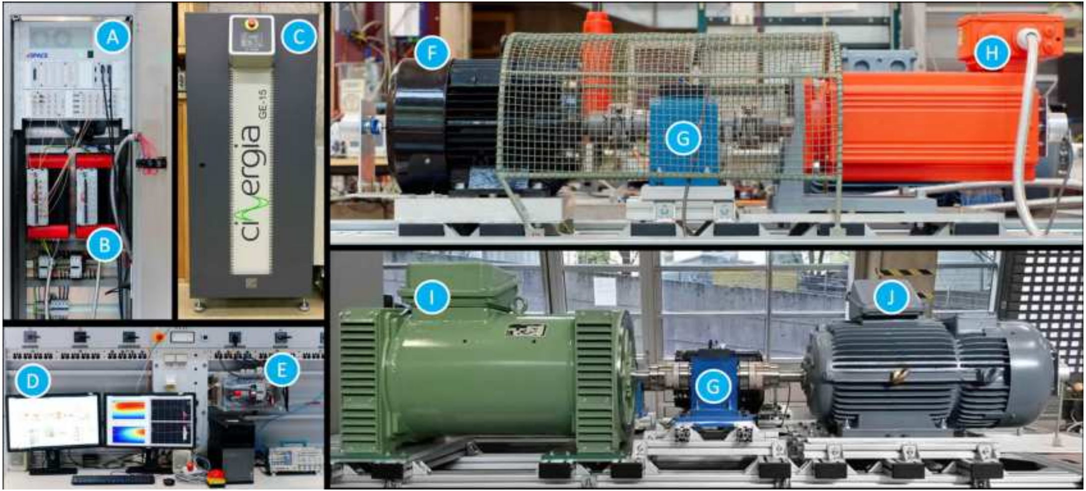

Outline

Introduction: Artificial intelligence (AI)

AI: Buzzwording and bullshitting? Even here?

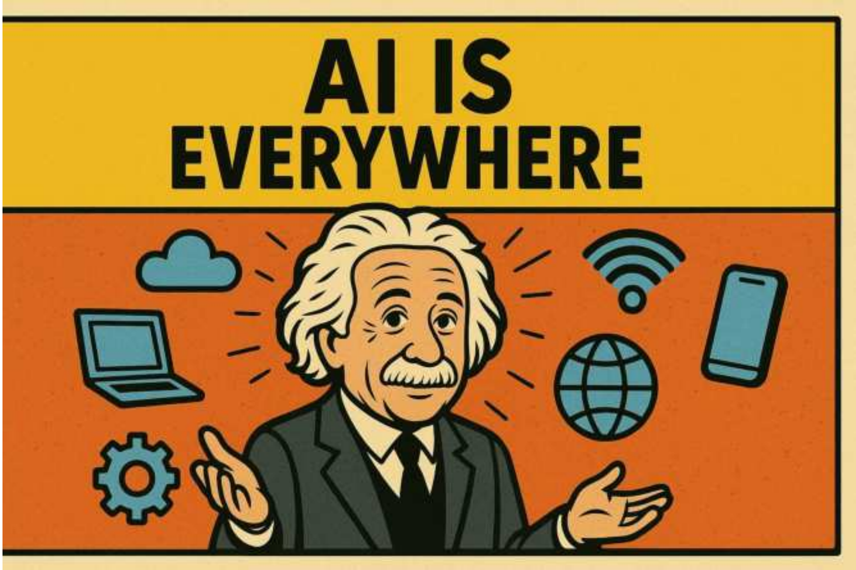

Introduction: Artificial intelligence (AI)

Comprehensive overview of AI in electrical drives [166, 167] (> 250 references)

IEEE Open Journal of Industry Applications

Received 20 February 2023; revised 9 May 2023; accepted 22 May 2023. Date of publication 9 June 2023;
date of current version 23 June 2023. The review of this article was arranged by Associate Editor M. Di Nardo.

Digital Object Identifier 10.1109/OJIA.2023.3284717

Machine Learning for the Control and Monitoring of Electric Machine Drives: Advances and Trends

SHEN ZHANG [1] (Member, IEEE), OLIVER WALLSCHEID [2] (Senior Member, IEEE), AND MARIO PORRMANN [3] (Member, IEEE)

[1] Joby Aviation, San Carlos, CA 94070 USA
[2] Department of Power Electronics and Electrical Drives, Paderborn University, 33098 Paderborn, Germany
[3] Institute of Computer Science, Osnabrück University, 49090 Osnabrück, Germany

CORRESPONDING AUTHOR: SHEN ZHANG (e-mail: shenzhang@gatech.edu)

This work was supported by the German Research Foundation (DFG) under Grant 459524199.

ABSTRACT This review article systematically summarizes the existing literature on utilizing machine learn-

Introduction: Artificial intelligence (AI)

Common applications of AI in electrical drives [24, 166–169]

AI-based or Artificial Neural Network (ANN)-based ...

- design
- modeling
- identification
- control
- observation
- FDD
- OPP
- ...

Introduction: Artificial intelligence (AI)

Additional materials

Besides symposium slides, following references may be of help:

[1] C.C. Aggarwal, *Neural Networks and Deep Learning: A Textbook*. Springer International Publishing: Cham, Switzerland, 2018 (https://link.springer.com/book/10.1007/978-3-319-94463-0).

[2] D. Schröder and M. Buss, *Intelligente Verfahren – Identifikation und Regelung nichtlinearer Systeme*. Springer-Verlag, 2017 (https://link.springer.com/book/10.1007/978-3-662-55327-5).

[3] S. Zhang, *Artificial Intelligence in Electric Machine Drives: Advances and Trends*. Techrxiv, 2022 (https://www.techrxiv.org/articles/preprint/Artificial_Intelligence_in_Electric_Machine_Drives_Advances_and_Trends/16782748https://doi.org/10.36227/techrxiv.16782748.v1)

[4] M. Zhang, O. Wallscheid and M. Porrmann, *Machine Learning for the Control and Monitoring of Electric Machine Drives: Advances and Trends*. IEEE Open Journal of Industry Applications, 2023 (https://doi.org/10.1109/OJIA.2023.3284717).

[5] M.A. Buettner, N. Monzen and C.M. Hackl, *Artificial Neural Network Based Optimal Feedforward Torque Control of Interior Permanent Magnet Synchronous Machines: A Feasibility Study and Comparison with the State-of-the-Art*. MDPI Energies, 2022 (https://doi.org/10.3390/en15051838).

Introduction: Artificial intelligence (AI)

Interesting podcast about AI in general: “Robot Brains” Podcast by Pieter Abbeel

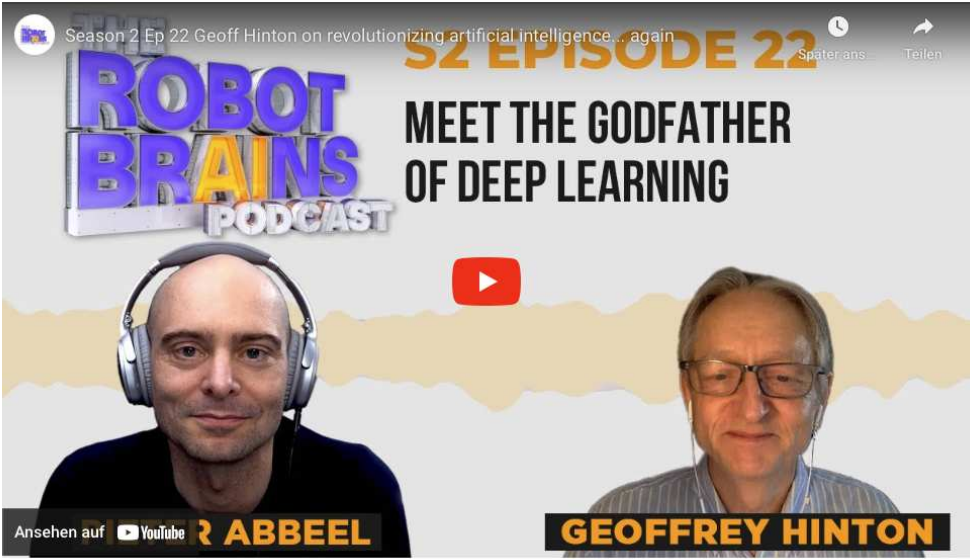

Outline

Outline

Preliminaries: The approximation problem

Problem statement (illustration)

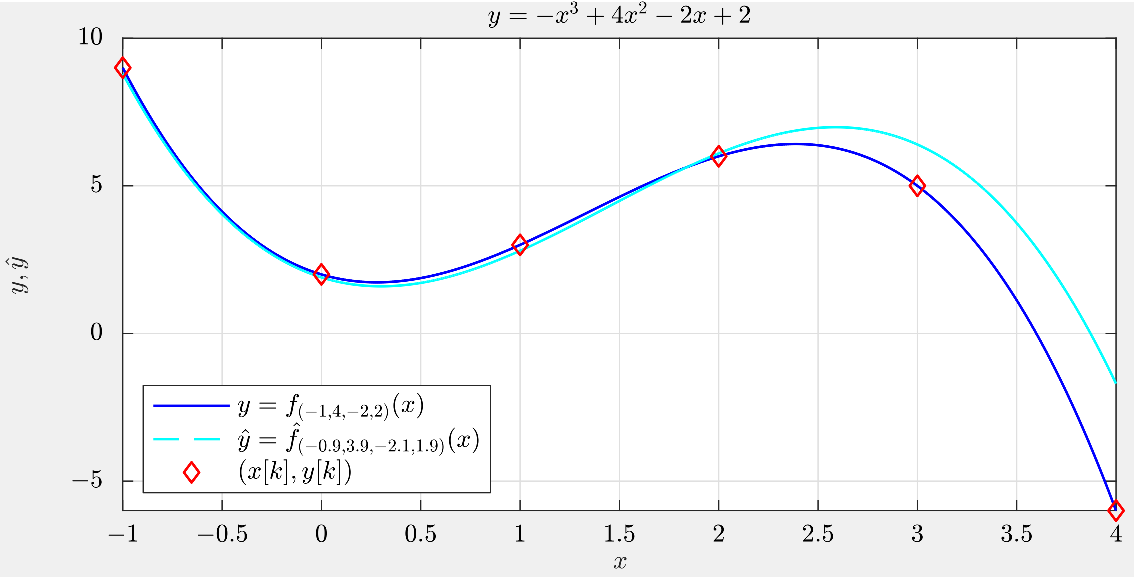

Preliminaries: The approximation problem

Problem statement (formal description)

The unknown function $\boldsymbol{f}_{\boldsymbol{\theta}} : \mathbb{R}^m \to \mathbb{R}^n$ with unknown parametrization $\boldsymbol{\theta} \in \mathbb{R}^p$, $p \in \mathbb{N}$, mapping

$$\boldsymbol{x} := (x_1, \ldots, x_m)^\top \mapsto \boldsymbol{y} := (y_1, \ldots, y_n)^\top := \boldsymbol{f}_{\boldsymbol{\theta}}(\boldsymbol{x}) \tag{1}$$

shall be approximated by a known function $\widehat{\boldsymbol{f}}_{\widehat{\boldsymbol{\theta}}} : \mathbb{R}^m \to \mathbb{R}^n$, with unknown parametrization $\widehat{\boldsymbol{\theta}} \in \mathbb{R}^{\hat{p}}$, $\hat{p} \in \mathbb{N}$, mapping

$$\boldsymbol{x} := (x_1, \ldots, x_m)^\top \mapsto \widehat{\boldsymbol{y}} := (\widehat{y}_1, \ldots, \widehat{y}_n)^\top := \widehat{\boldsymbol{f}}_{\widehat{\boldsymbol{\theta}}}(\boldsymbol{x}) \approx \boldsymbol{f}_{\boldsymbol{\theta}}(\boldsymbol{x}). \tag{2}$$

Example 0

Consider

(a) $y = f_{\boldsymbol{\theta}}(x) = \theta_1 x^2 + \theta_2$ and $\widehat{y} = \widehat{f}_{\widehat{\boldsymbol{\theta}}}(x) = \widehat{\theta}_1 x^2 + \widehat{\theta}_2 x + \widehat{\theta}_3$ or

(b) $y = f_{\boldsymbol{\theta}}(x_1, x_2) = \theta_1 x_1^2 + \theta_2 x_2 + \theta_3$ and $\widehat{y} = \widehat{f}_{\widehat{\boldsymbol{\theta}}}(x_1, x_2) = \widehat{\theta}_1 x_1^3 + \widehat{\theta}_2 x_1^2 + \widehat{\theta}_3 x_2^2 + \widehat{\theta}_4$.

What can we observe? Which problems may arise?

Preliminaries: The approximation problem

Problem statement

The unknown function $\boldsymbol{f}_{\boldsymbol{\theta}} : \mathbb{R}^m \to \mathbb{R}^n$ with unknown parametrization $\boldsymbol{\theta} \in \mathbb{R}^p$, $p \in \mathbb{N}$, mapping

$$\boldsymbol{x} := (x_1, \ldots, x_m)^\top \mapsto \boldsymbol{y} := (y_1, \ldots, y_n)^\top := \boldsymbol{f}_{\boldsymbol{\theta}}(\boldsymbol{x}) \tag{3}$$

shall be approximated by a known function $\widehat{\boldsymbol{f}}_{\widehat{\boldsymbol{\theta}}} : \mathbb{R}^m \to \mathbb{R}^n$, with unknown parametrization $\widehat{\boldsymbol{\theta}} \in \mathbb{R}^{\hat{p}}$, $\hat{p} \in \mathbb{N}$, mapping

$$\boldsymbol{x} := (x_1, \ldots, x_m)^\top \mapsto \widehat{\boldsymbol{y}} := (\widehat{y}_1, \ldots, \widehat{y}_n)^\top := \widehat{\boldsymbol{f}}_{\widehat{\boldsymbol{\theta}}}(\boldsymbol{x}) \approx \boldsymbol{f}_{\boldsymbol{\theta}}(\boldsymbol{x}). \tag{4}$$

Remark 1

Best-case: (motivates for structered or physics-informed ANNs, e.g. flux linkage prototype functions)
- $\boldsymbol{f}_{\boldsymbol{\theta}}(\boldsymbol{x}) = \widehat{\boldsymbol{f}}_{\boldsymbol{\theta}}(\boldsymbol{x})$ (functions equal for same parametrization) and
- $\boldsymbol{\theta} = \widehat{\boldsymbol{\theta}}$ (parametrizations equal, including $p = \widehat{p}$).

Worst-case: (usual case to be dealt with!)
- $\boldsymbol{f}_{\boldsymbol{\theta}}(\boldsymbol{x}) \neq \widehat{\boldsymbol{f}}_{\boldsymbol{\theta}}(\boldsymbol{x})$ (functions not equal for same parametrization) and
- $\boldsymbol{\theta} \neq \widehat{\boldsymbol{\theta}}$ (parametrizations not equal, including $p \neq \widehat{p}$).

Preliminaries: The approximation problem

Principle solution approach

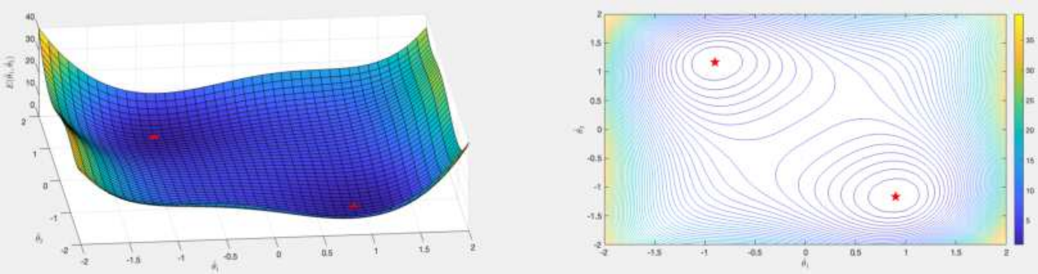

Approximation error vector

$$\boldsymbol{e} := \boldsymbol{y} - \widehat{\boldsymbol{y}} = \boldsymbol{y} - \widehat{\boldsymbol{f}}_{\widehat{\boldsymbol{\theta}}}(\boldsymbol{x}) \in \mathbb{R}^n$$

Error surface (e.g., squared error or Mean Squared Error (MSE))

$$E\colon \mathbb{R}^{\widehat{p}} \to \mathbb{R}, \quad \widehat{\boldsymbol{\theta}} \mapsto E(\widehat{\boldsymbol{\theta}}) := E(\widehat{\boldsymbol{\theta}}, \boldsymbol{y}, \boldsymbol{x}) := \tfrac{1}{2}\boldsymbol{e}^\top \boldsymbol{e} = \tfrac{1}{2}\left[\boldsymbol{y}^\top \boldsymbol{y} - 2\boldsymbol{y}^\top \widehat{\boldsymbol{f}}_{\widehat{\boldsymbol{\theta}}}(\boldsymbol{x}) + \widehat{\boldsymbol{f}}_{\widehat{\boldsymbol{\theta}}}(\boldsymbol{x})^\top \widehat{\boldsymbol{f}}_{\widehat{\boldsymbol{\theta}}}(\boldsymbol{x})\right]$$

Goal: Solve optimization problem to find minimizer $\widehat{\boldsymbol{\theta}}^\star$ ($\bigstar$)

$$\widehat{\boldsymbol{\theta}}^\star := \arg\min_{\widehat{\boldsymbol{\theta}}} E(\widehat{\boldsymbol{\theta}})$$

Preliminaries: The approximation problem

Typical challenges during optimization: “Wrong” initialization $\Rightarrow$ global minmum not reached [170, Abb. 4.12])

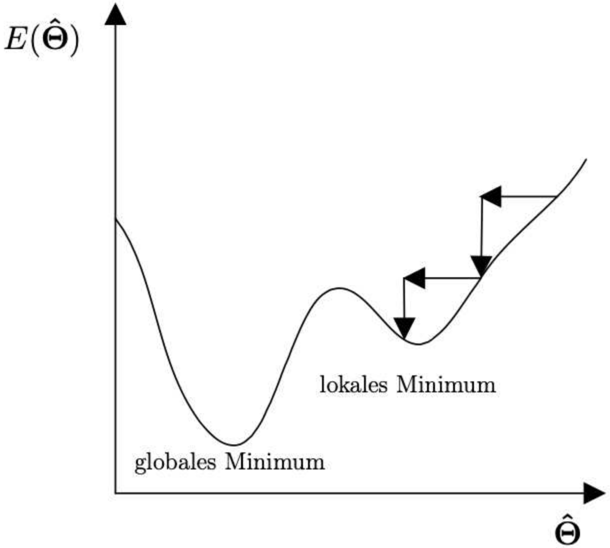

Preliminaries: The approximation problem

Typical challenges during optimization: Flat plateaus $\Rightarrow$ no progress [170, Abb. 4.13]

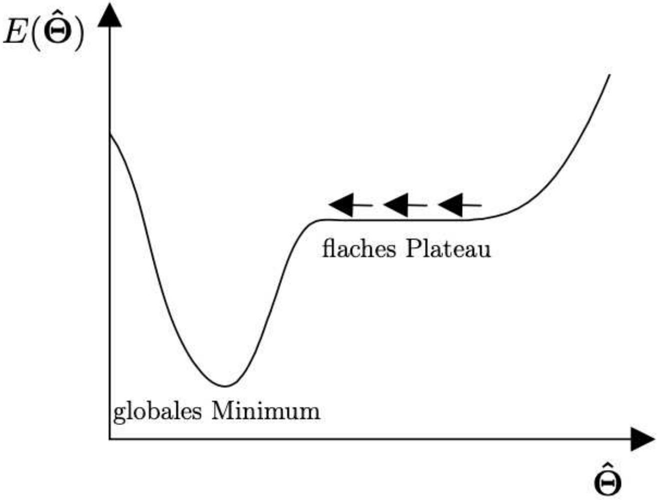

Preliminaries: The approximation problem

Typical challenges during optimization: Non-convergence (e.g., oscillations) [170, Abb. 4.14]

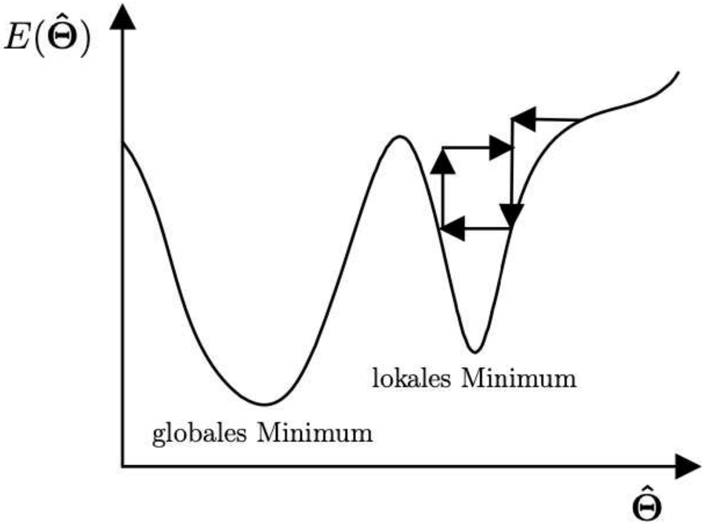

Preliminaries: The approximation problem

Typical challenges during optimization

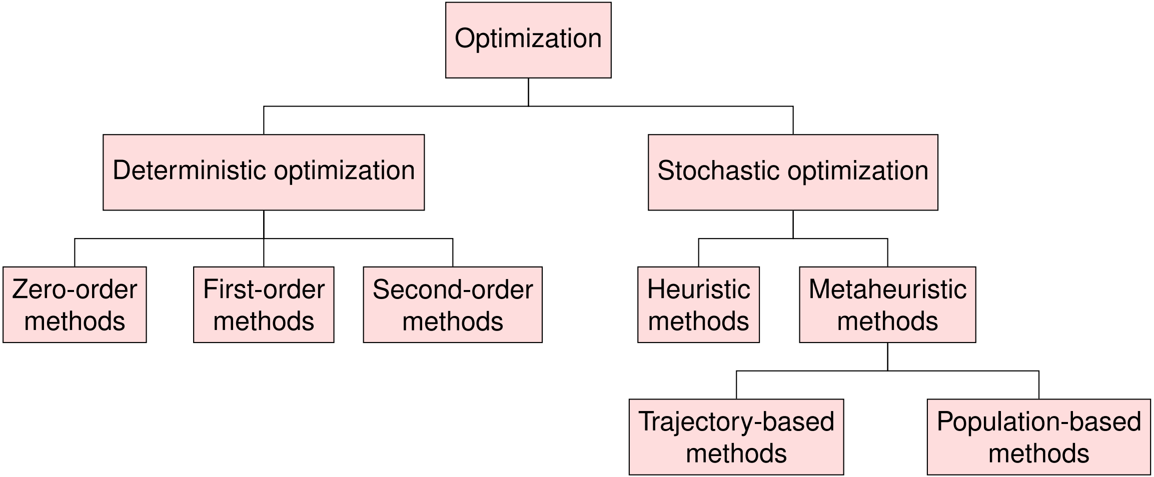

For more details, see [170, Chapter 10 & 11] or [171, Chapter 3] or https://en.wikipedia.org/wiki/Global_optimization.

Preliminaries: The approximation problem

Deterministic optimization: Optimality conditions

Necessary condition:

$$\begin{aligned}
\boldsymbol{0}_{\hat{p}} \overset{!}{=} \frac{\mathrm{d}E(\widehat{\boldsymbol{\theta}})}{\mathrm{d}\widehat{\boldsymbol{\theta}}} &= -\frac{\mathrm{d}\widehat{\boldsymbol{f}}_{\widehat{\boldsymbol{\theta}}}(\boldsymbol{x})}{\mathrm{d}\widehat{\boldsymbol{\theta}}}^{\top}\boldsymbol{y} + \frac{1}{2}\left[\frac{\mathrm{d}\widehat{\boldsymbol{f}}_{\widehat{\boldsymbol{\theta}}}(\boldsymbol{x})}{\mathrm{d}\widehat{\boldsymbol{\theta}}}^{\top}\widehat{\boldsymbol{f}}_{\widehat{\boldsymbol{\theta}}}(\boldsymbol{x}) + \widehat{\boldsymbol{f}}_{\widehat{\boldsymbol{\theta}}}(\boldsymbol{x})^{\top}\frac{\mathrm{d}\widehat{\boldsymbol{f}}_{\widehat{\boldsymbol{\theta}}}(\boldsymbol{x})}{\mathrm{d}\widehat{\boldsymbol{\theta}}^{\top}}\right] \\
&= -\frac{\mathrm{d}\widehat{\boldsymbol{f}}_{\widehat{\boldsymbol{\theta}}}(\boldsymbol{x})}{\mathrm{d}\widehat{\boldsymbol{\theta}}}^{\top}\left(\boldsymbol{y} - \widehat{\boldsymbol{f}}_{\widehat{\boldsymbol{\theta}}}(\boldsymbol{x})\right) \\
&= \boxed{-\underbrace{\frac{\mathrm{d}\widehat{\boldsymbol{f}}_{\widehat{\boldsymbol{\theta}}}(\boldsymbol{x})}{\mathrm{d}\widehat{\boldsymbol{\theta}}}^{\top}}_{=:\boldsymbol{J}_{\widehat{\boldsymbol{f}}}^{\top}\in\mathbb{R}^{\hat{p}\times n}}\boldsymbol{e} =: \boldsymbol{g}_E \in \mathbb{R}^{\hat{p}} \text{ (gradient of } E \text{ with Jacobian } \boldsymbol{J}_{\widehat{\boldsymbol{f}}} \text{ of } \widehat{\boldsymbol{f}}\text{)}} \qquad (5)
\end{aligned}$$

Sufficient condition:

$$\begin{aligned}
0 \overset{!}{<} \frac{\mathrm{d}}{\mathrm{d}\widehat{\boldsymbol{\theta}}^{\top}}\frac{\mathrm{d}E(\widehat{\boldsymbol{\theta}})}{\mathrm{d}\widehat{\boldsymbol{\theta}}} &= -\frac{\mathrm{d}}{\mathrm{d}\widehat{\boldsymbol{\theta}}^{\top}}\left[\boldsymbol{J}_{\widehat{\boldsymbol{f}}}^{\top}\left(\boldsymbol{y} - \widehat{\boldsymbol{f}}_{\widehat{\boldsymbol{\theta}}}(\boldsymbol{x})\right)\right] = -\frac{\mathrm{d}}{\mathrm{d}\widehat{\boldsymbol{\theta}}^{\top}}\left[\boldsymbol{J}_{\widehat{\boldsymbol{f}}}^{\top}\boldsymbol{e}\right] - \boldsymbol{J}_{\widehat{\boldsymbol{f}}}^{\top}\frac{\mathrm{d}}{\mathrm{d}\widehat{\boldsymbol{\theta}}^{\top}}\left[\boldsymbol{y} - \widehat{\boldsymbol{f}}_{\widehat{\boldsymbol{\theta}}}(\boldsymbol{x})\right] \\
&= \boxed{-\frac{\mathrm{d}}{\mathrm{d}\widehat{\boldsymbol{\theta}}^{\top}}\left[\boldsymbol{J}_{\widehat{\boldsymbol{f}}}^{\top}\boldsymbol{e}\right] + \boldsymbol{J}_{\widehat{\boldsymbol{f}}}^{\top}\boldsymbol{J}_{\widehat{\boldsymbol{f}}} =: \boldsymbol{H}_E \in \mathbb{R}^{\hat{p}\times\hat{p}} \quad \text{(Hessian of } E\text{)}} \qquad (6)
\end{aligned}$$

Preliminaries: The approximation problem

Parameter adaption: Derivation of general adaption law

Error surface approximation (Taylor expansion)

$$E(\widehat{\boldsymbol{\theta}} + \Delta\widehat{\boldsymbol{\theta}}) \approx E(\widehat{\boldsymbol{\theta}}) + \boldsymbol{g}_E^\top \Delta\widehat{\boldsymbol{\theta}} + \tfrac{1}{2}\Delta\widehat{\boldsymbol{\theta}}^\top \boldsymbol{H}_E \Delta\widehat{\boldsymbol{\theta}}$$

which we want to minimize with respect to $\Delta\widehat{\boldsymbol{\theta}} := \widehat{\boldsymbol{\theta}}[b+1] - \widehat{\boldsymbol{\theta}}[b]$ ("b-th batch"), i.e.

$$\frac{\mathrm{d}E(\widehat{\boldsymbol{\theta}} + \Delta\widehat{\boldsymbol{\theta}})}{\mathrm{d}\Delta\widehat{\boldsymbol{\theta}}} \approx \boldsymbol{g}_E + \boldsymbol{H}_E \Delta\widehat{\boldsymbol{\theta}} \overset{!}{=} \boldsymbol{0}_{\widehat{p}} \iff \Delta\widehat{\boldsymbol{\theta}} = -\boldsymbol{H}_E^{-1}\boldsymbol{g}_E = \boldsymbol{H}_E^{-1}\boldsymbol{J}_{\widehat{\boldsymbol{f}}}^\top \boldsymbol{e}, \tag{7}$$

from which a **general parameter adaption** law can be deduced (if problem is convex)

$$\widehat{\boldsymbol{\theta}}[b+1] = \widehat{\boldsymbol{\theta}}[b] - \boldsymbol{H}_E^{-1}\boldsymbol{g}_E = \widehat{\boldsymbol{\theta}}[b] + \boldsymbol{H}_E^{-1}\boldsymbol{J}_{\widehat{\boldsymbol{f}}}^\top \boldsymbol{e}[b]$$

Preliminaries: The approximation problem

Parameter adaption: Different approximations of $\boldsymbol{H}_E^{-1}$ yield different parameter adaption laws (all following $\mu \in (0,1]$)

- **Gradient descent (GD)**:

$$\boldsymbol{H}_E^{-1} \approx \mu_{\mathrm{GD}}[b] \Longrightarrow \widehat{\boldsymbol{\theta}}[b+1] = \widehat{\boldsymbol{\theta}}[b] + \mu_{\mathrm{GD}}[b]\boldsymbol{J}_{\widehat{\boldsymbol{f}}}^\top \boldsymbol{e}[b]$$

- **Gradient descent with weighted momentum term (MT)**:

$$\boldsymbol{H}_E^{-1} \approx \mu_{\mathrm{GD}}[b] \ \&\ \mu_{\mathrm{MT}}[b]\big(\widehat{\boldsymbol{\theta}}[b] - \widehat{\boldsymbol{\theta}}[b-1]\big) \Longrightarrow \widehat{\boldsymbol{\theta}}[b+1] = \widehat{\boldsymbol{\theta}}[b] + \mu_{\mathrm{GD}}[b]\boldsymbol{J}_{\widehat{\boldsymbol{f}}}^\top \boldsymbol{e}[b] + \mu_{\mathrm{MT}}[b]\big(\widehat{\boldsymbol{\theta}}[b] - \widehat{\boldsymbol{\theta}}[b-1]\big)$$

- **Newton method (NM)**:

$$\boldsymbol{H}_E^{-1} \approx \mu_{\mathrm{NM}}[b]\boldsymbol{H}_E^{-1} \Longrightarrow \widehat{\boldsymbol{\theta}}[b+1] = \widehat{\boldsymbol{\theta}}[b] + \mu_{\mathrm{NM}}[b]\boldsymbol{H}_E^{-1}\boldsymbol{J}_{\widehat{\boldsymbol{f}}}^\top \boldsymbol{e}[b]$$

- **Gauss-Newton method (GN)**:

$$\boldsymbol{H}_E^{-1} \approx \mu_{\mathrm{GN}}[b]\boldsymbol{J}_{\widehat{\boldsymbol{f}}}^\top \boldsymbol{J}_{\widehat{\boldsymbol{f}}} \Longrightarrow \widehat{\boldsymbol{\theta}}[b+1] = \widehat{\boldsymbol{\theta}}[b] + \mu_{\mathrm{GN}}[b](\boldsymbol{J}_{\widehat{\boldsymbol{f}}}^\top \boldsymbol{J}_{\widehat{\boldsymbol{f}}})^{-1}\boldsymbol{J}_{\widehat{\boldsymbol{f}}}^\top \boldsymbol{e}[b]$$

- **Levenberg-Marquardt (LM)**:

$$\boldsymbol{H}_E^{-1} \approx \left[\boldsymbol{J}_{\widehat{\boldsymbol{f}}}^\top \boldsymbol{J}_{\widehat{\boldsymbol{f}}} + \mu_{\mathrm{LM}}[b]\boldsymbol{I}_{\widehat{p}}\right] \Longrightarrow \widehat{\boldsymbol{\theta}}[b+1] = \widehat{\boldsymbol{\theta}}[b] + \left[\boldsymbol{J}_{\widehat{\boldsymbol{f}}}^\top \boldsymbol{J}_{\widehat{\boldsymbol{f}}} + \mu_{\mathrm{LM}}[b]\boldsymbol{I}_{\widehat{p}}\right]^{-1}\boldsymbol{J}_{\widehat{\boldsymbol{f}}}^\top \boldsymbol{e}[b]$$

- **modified Levenberg-Marquardt (mLM; Fletcher 1971)**:

$$\boldsymbol{H}_E^{-1} \approx \left[\boldsymbol{J}_{\widehat{\boldsymbol{f}}}^\top \boldsymbol{J}_{\widehat{\boldsymbol{f}}} + \mu_{\mathrm{mLM}}[b]\,\mathrm{diag}(\boldsymbol{J}_{\widehat{\boldsymbol{f}}}^\top \boldsymbol{J}_{\widehat{\boldsymbol{f}}})\right] \Longrightarrow \widehat{\boldsymbol{\theta}}[b+1] = \widehat{\boldsymbol{\theta}}[b] + \left[\boldsymbol{J}_{\widehat{\boldsymbol{f}}}^\top \boldsymbol{J}_{\widehat{\boldsymbol{f}}} + \mu_{\mathrm{mLM}}[b]\,\mathrm{diag}(\boldsymbol{J}_{\widehat{\boldsymbol{f}}}^\top \boldsymbol{J}_{\widehat{\boldsymbol{f}}})\right]^{-1}\boldsymbol{J}_{\widehat{\boldsymbol{f}}}^\top \boldsymbol{e}[b]$$

- ... (for more adaption laws and stochastic approaches, see [170, Chapter 10 & 11] or [171, Chapter 3])

Outline

Preliminaries: Artificial neural networks (ANNs)

Motivation and analogy to human nervous system [171, Fig. 1.1]

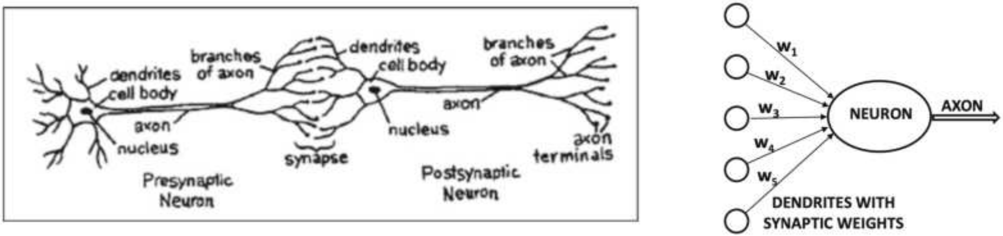

(a) Biological neural network (b) Artificial neural network

Figure 1.1: The synaptic connections between neurons. The image in (a) is from "*The Brain: Understanding Neurobiology Through the Study of Addiction* [598]." Copyright ©2000 by BSCS & Videodiscovery. All rights reserved. Used with permission.

Preliminaries: Artificial neural networks (ANNs)

Typical ANN structure with $m = m_1$ inputs, L layers ($L-2$ hidden layers) & $n = m_L$ outputs

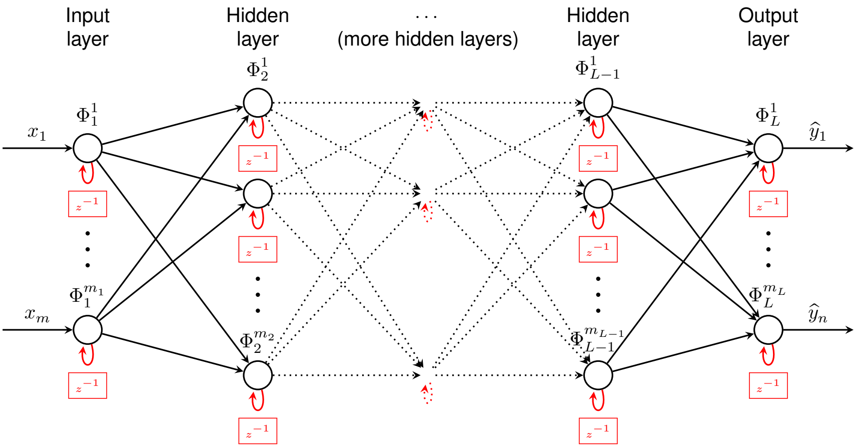

Artificial Neural Network (ANN; w/o red loops) or **Recurrent Neural Network** (RNN; w/ red loops including unit delay z^{-1} for estimation of dynamics as well). The l-th layer has m_l inputs and m_l neurons with activation functions $\Phi_l^1, \ldots \Phi_l^{m_l}$ feeding m_{l+1} neurons of the $l+1$-th layer.

Preliminaries: Artificial neural networks (ANNs)

ANN properties [170]

(P_1) **Representation capability** means that the chosen network topology with the chosen activation functions is capable of fulfilling the approximation task. $\Longrightarrow$ *Proper choice of topology and activation functions is crucial (e.g., structered or physics-informed ANN design)!*

(P_2) **Learning capability** describes the learning process by which the parameters of an ANN are adapted by an appropriate learning method, such that it exhibits the desired approximation later during validation and test phases. In practice, criteria such as learning speed, convergence, parameter uniqueness, stability, and online capability of the learning method play an important role. $\Longrightarrow$ *Proper choice of learning method (deterministic vs. stochastic) is crucial!*

(P_3) **Generalization capability** describes the ability of the trained ANN to accurately represent value pairs that are not included in the training set during the validation and test phases. Specifically, it distinguishes between interpolation and extrapolation behavior, which characterize the network's approximation capability within and outside the input range of the training data. $\Longrightarrow$ *Validation (parallel to training) and proper choice of input data (e.g., Latin Hyper Cube Sampling) is crucial!*

Remark 2 (Universal approximation theory [172])

For any $\boldsymbol{f}_{\boldsymbol{\theta}}(\cdot) \in \mathcal{C}^1(K; \mathbb{R}^n)$ with compact set $K \subset \mathbb{R}^m$ and any $\varepsilon > 0$, there exists an artificial neural network (ANN) such that $\|\boldsymbol{f}_{\boldsymbol{\theta}} - \widehat{\boldsymbol{f}}_{\hat{\boldsymbol{\theta}}}\|_\infty < \varepsilon$.

Preliminaries: Artificial neural networks (ANNs)

Artificial neurons: Illustration of i-th artificial neuron in the l-th layer

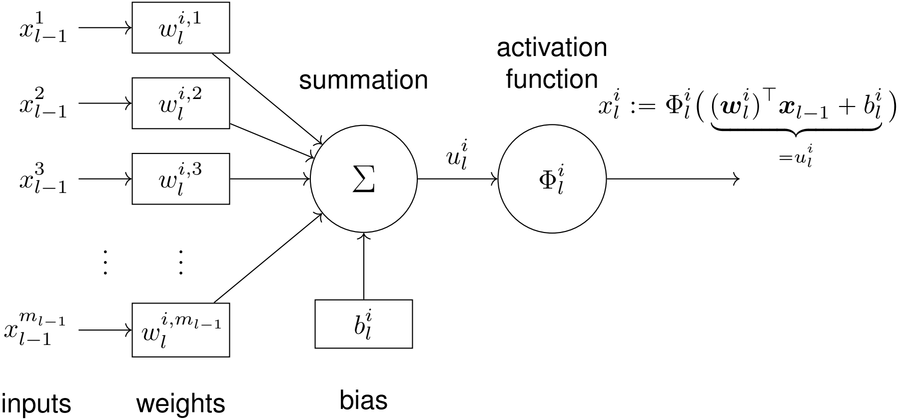

Remark 3

The neuron's weighted and biased input is $u_l^i := (\boldsymbol{w}_l^i)^\top \boldsymbol{x}_{l-1} + b_l^i \in \mathbb{R}$ with input $\boldsymbol{x}_{l-1} := (x_{l-1}^1, \ldots, x_{l-1}^{m_{l-1}})^\top \in \mathbb{R}^{m_{l-1}}$, weights $\boldsymbol{w}_l^i := (w_l^{i,1}, \ldots, w_l^{i,m_{l-1}})^\top \in \mathbb{R}^{m_{l-1}}$ and bias $b_l^i \in \mathbb{R}$.

Preliminaries: Artificial neural networks (ANNs)

Artificial neurons: Illustration of typical activation functions

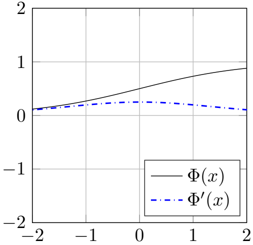

(a) Sigmoid $\Phi_{\mathrm{sig}}(x)$.

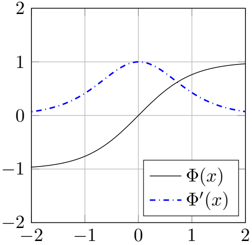

(b) Tangens hyperbolicus $\Phi_{\mathrm{tanh}}(x)$.

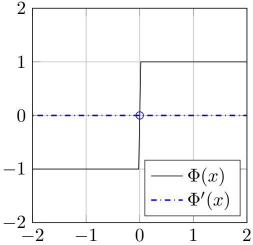

(c) Signum (sign) $\Phi_{\mathrm{sgn}}(x)$.

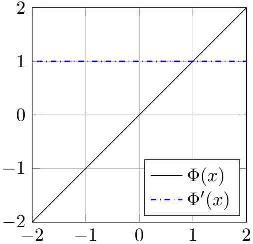

(d) Identity $\Phi_{\mathrm{id}}(x)$.

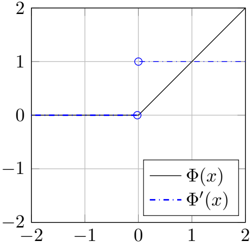

(e) **Rectified Linear Unit** $\Phi_{\mathrm{ReLU}}(x)$.

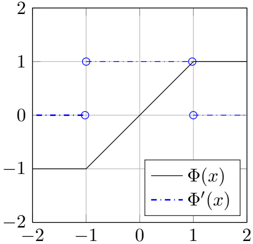

(f) Saturation $\Phi_{\mathrm{sat}}(x)$.

Preliminaries: Artificial neural networks (ANNs)

ANN output: Recursive definition

For an ANN with L layers (i.e. one input layer, one output layer and $L-2$ hidden layers), its output is **recursively** defined and given by

$$\hat{\boldsymbol{y}} = \boldsymbol{\Phi}_L\Bigg(\overbrace{\boldsymbol{W}_L \underbrace{\boldsymbol{\Phi}_{L-1}\Bigg(\overbrace{\boldsymbol{W}_{L-1}\underbrace{\boldsymbol{\Phi}_{L-2}\Bigg(\cdots \underbrace{\boldsymbol{\Phi}_2\Bigg(\overbrace{\boldsymbol{W}_2\underbrace{\boldsymbol{\Phi}_1\Big(\overbrace{\boldsymbol{W}_1\boldsymbol{x}+\boldsymbol{b}_1}^{=:\boldsymbol{u}_1}\Big)}_{=:\boldsymbol{x}_1}+\boldsymbol{b}_2}^{=:\boldsymbol{u}_2}\Bigg)}_{=:\boldsymbol{x}_2}\Bigg)}_{\vdots}+\boldsymbol{b}_{L-1}}^{\vdots}\Bigg)}_{=:\boldsymbol{x}_{L-1}}+\boldsymbol{b}_L}^{=:\boldsymbol{u}_L}\Bigg). \tag{8}$$

Please note that per definition, $\boldsymbol{x} =: \boldsymbol{x}_0$ with dimensions $m =: m_0$ represents the input to the (first) input layer.

Preliminaries: Artificial neural networks (ANNs)

Representing ANNs as parametrized functions: Rewriting the neuron input vector

Rewriting the weighted and biased (but not activated) input $\boldsymbol{u}_l$ bof the l-th layer as

$$\boldsymbol{u}_l := \boldsymbol{W}_l \boldsymbol{x}_{l-1} + \boldsymbol{b}_l = \begin{pmatrix} (\boldsymbol{w}_l^1)^\top \boldsymbol{x}_{l-1} + b_l^1 \\ \vdots \\ (\boldsymbol{w}_l^{m_l})^\top \boldsymbol{x}_{l-1} + b_l^{m_l} \end{pmatrix} \tag{9}$$

$$= \underbrace{\begin{bmatrix} \boldsymbol{x}_{l-1}^\top & \boldsymbol{0}_{m_{l-1}}^\top & \dots & \boldsymbol{0}_{m_{l-1}}^\top & 1 & 0 & \dots & 0 \\ \boldsymbol{0}_{m_{l-1}}^\top & \boldsymbol{x}_{l-1}^\top & \dots & \boldsymbol{0}_{m_{l-1}}^\top & 0 & 1 & \dots & 0 \\ & & \ddots & & & & \ddots & \\ \boldsymbol{0}_{m_{l-1}}^\top & \boldsymbol{0}_{m_{l-1}}^\top & \dots & \boldsymbol{x}_{l-1}^\top & 0 & 0 & \dots & 1 \end{bmatrix}}_{=: \boldsymbol{X}_{l-1}^\top \in \mathbb{R}^{m_l \times m_l \cdot (m_{l-1}+1)}} \underbrace{\begin{pmatrix} \boldsymbol{w}_l^1 \\ \vdots \\ \boldsymbol{w}_l^{m_l} \\ \boldsymbol{b}_l \end{pmatrix}}_{=: \widehat{\boldsymbol{\theta}}_l \in \mathbb{R}^{\widehat{p}_l}}, \tag{10}$$

where $\widehat{\boldsymbol{\theta}}_l \in \mathbb{R}^{\widehat{p}_l}$ comprises all parameters (weights and biases) of the l-th layer, with $\widehat{p}_l := m_l \cdot (m_{l-1} + 1)$,

Preliminaries: Artificial neural networks (ANNs)

Representing ANNs as parametrized functions: Rewriting the neuron input vector (cont'd)

yields

$$\widehat{\boldsymbol{y}} = \boldsymbol{\Phi}_L\Bigg(\boldsymbol{W}_L\,\boldsymbol{\Phi}_{L-1}\Bigg(\boldsymbol{W}_{L-1}\,\boldsymbol{\Phi}_{L-2}\Bigg(\cdots\underbrace{\boldsymbol{\Phi}_2\Bigg(\boldsymbol{W}_2\underbrace{\boldsymbol{\Phi}_1\Bigg(\boldsymbol{W}_1\boldsymbol{x}+\boldsymbol{b}_1\Bigg)}_{=:\boldsymbol{x}_1=\boldsymbol{\Phi}_1(\boldsymbol{X}_0^\top\widehat{\boldsymbol{\theta}}_1)}+\boldsymbol{b}_2\Bigg)}_{=:\boldsymbol{x}_2=\boldsymbol{\Phi}_2(\boldsymbol{X}_1^\top\widehat{\boldsymbol{\theta}}_2)\quad\vdots}\Bigg)+\boldsymbol{b}_{L-1}\Bigg)+\boldsymbol{b}_L\Bigg)$$

$$\underbrace{\quad}_{=:\boldsymbol{x}_{L-2}=\boldsymbol{\Phi}_{L-2}(\boldsymbol{X}_{L-3}^\top\widehat{\boldsymbol{\theta}}_{L-2})}\qquad \underbrace{\quad}_{=:\boldsymbol{x}_{L-1}=\boldsymbol{\Phi}_{L-1}(\boldsymbol{X}_{L-2}^\top\widehat{\boldsymbol{\theta}}_{L-1})}$$

$$\begin{aligned} &= \boldsymbol{\Phi}_L(\boldsymbol{X}_{L-1}^\top\widehat{\boldsymbol{\theta}}_L) \\ &=: \widehat{\boldsymbol{f}}_{\widehat{\boldsymbol{\theta}}}(\boldsymbol{x}) \end{aligned} \tag{11}$$

with all $\widehat{p}$ parameters (weights and biases) of the ANN collected in

$$\widehat{\boldsymbol{\theta}} := (\widehat{\boldsymbol{\theta}}_1^\top, \widehat{\boldsymbol{\theta}}_2^\top, \ldots, \widehat{\boldsymbol{\theta}}_L^\top)^\top \in \mathbb{R}^{\widehat{p}} \quad \text{where} \quad \widehat{p} := \sum_{l=1}^{L}\widehat{p}_l = \sum_{l=1}^{L} m_l\,(m_{l-1}+1).$$

Preliminaries: Artificial neural networks (ANNs)

Training (learning) and validation: Overview

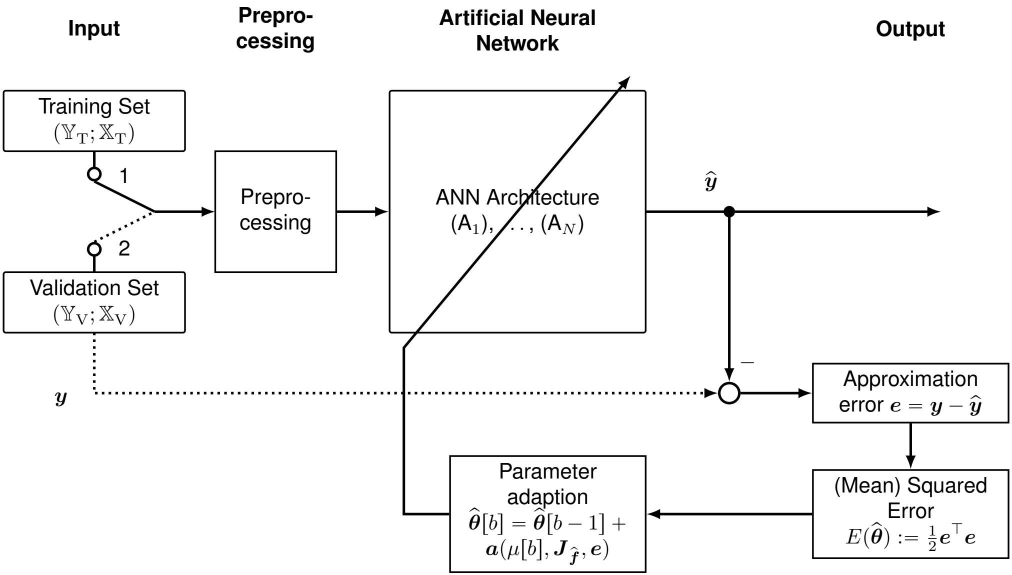

Preliminaries: Artificial neural networks (ANNs)

Training (learning) and validation: Adaption of ANN parameters (i.e., weights and biases)

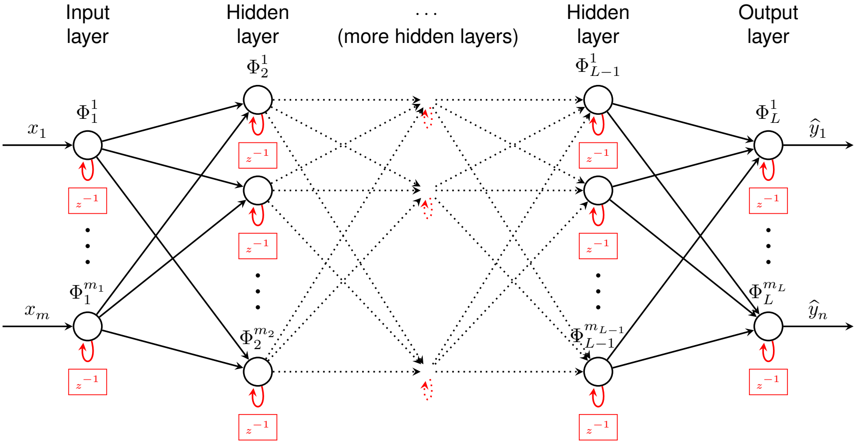

$\Longrightarrow$ How can we train the ANN and adapt its weights and biases? $\widehat{\boldsymbol{\theta}}[b] = \widehat{\boldsymbol{\theta}}[b-1] + \boldsymbol{a}(\mu[b], \boldsymbol{J}_{\hat{\boldsymbol{f}}}, \boldsymbol{e})$

$\Longrightarrow$ To do so, we need parameter adaptation (as introduced above) ... and **Backpropagation**!

Preliminaries: Artificial neural networks (ANNs)

Training (learning) and validation: Backpropagation

For number of outputs $n =: m_L$, number of inputs $m =: m_0$, number of parameters of l-th layer $\widehat{p}_l := m_l \cdot (m_{l-1} + 1)$ and number of all parameters $\widehat{p} := \sum_{l=1}^{L} \widehat{p}_l$, one obtains for each layers $l \in \{1, \ldots, L\}$ the **sub-Jacobian matrix**

$$
\begin{aligned}
\frac{\mathrm{d}\widehat{\boldsymbol{f}}_{\widehat{\boldsymbol{\theta}}}(\boldsymbol{x})}{\mathrm{d}\widehat{\boldsymbol{\theta}}_l^\top} &= \underbrace{\frac{\mathrm{d}\boldsymbol{\Phi}_L(\boldsymbol{u}_L)}{\mathrm{d}\boldsymbol{u}_L^\top}}_{\in\mathbb{R}^{m_L\times m_L}} \cdot \underbrace{\frac{\mathrm{d}\boldsymbol{u}_L}{\mathrm{d}\boldsymbol{x}_{L-1}^\top}}_{\in\mathbb{R}^{m_L\times m_{L-1}}} \cdot \underbrace{\frac{\mathrm{d}\boldsymbol{x}_{L-1}}{\mathrm{d}\boldsymbol{u}_{L-1}^\top}}_{\in\mathbb{R}^{m_{L-1}\times m_{L-1}}} \cdot \underbrace{\frac{\mathrm{d}\boldsymbol{u}_{L-1}}{\mathrm{d}\boldsymbol{x}_{L-2}^\top}}_{\in\mathbb{R}^{m_{L-1}\times m_{L-2}}} \cdot \ldots \cdot \underbrace{\frac{\mathrm{d}\boldsymbol{x}_l}{\mathrm{d}\boldsymbol{u}_l^\top}}_{\in\mathbb{R}^{m_l\times m_l}} \cdot \underbrace{\frac{\mathrm{d}\boldsymbol{u}_l}{\mathrm{d}\widehat{\boldsymbol{\theta}}_l^\top}}_{\in\mathbb{R}^{m_l\times \widehat{p}_l}} \\
&= \boldsymbol{\Phi}'_L \, \boldsymbol{W}_L \, \boldsymbol{\Phi}'_{L-1} \, \boldsymbol{W}_{L-1} \, \boldsymbol{\Phi}'_{L-2} \, \boldsymbol{W}_{L-2} \cdots \boldsymbol{\Phi}'_l \, \boldsymbol{X}_{l-1}^\top \in \mathbb{R}^{n\times\widehat{p}_l}.
\end{aligned}
\tag{12}
$$

Hence, **parameter adaption** (e.g., using Gradient Descent) is given by

$$
\widehat{\boldsymbol{\theta}}[b+1] := \underbrace{\begin{pmatrix} \widehat{\boldsymbol{\theta}}_1[b+1] \\ \vdots \\ \widehat{\boldsymbol{\theta}}_L[b+1] \end{pmatrix}}_{\in\mathbb{R}^{\widehat{p}}} = \widehat{\boldsymbol{\theta}}[b] + \mu_{\mathrm{GD}} \underbrace{\begin{pmatrix} \frac{\mathrm{d}\widehat{\boldsymbol{f}}_{\widehat{\boldsymbol{\theta}}}(\boldsymbol{x})}{\mathrm{d}\widehat{\boldsymbol{\theta}}_1}^\top \\ \vdots \\ \frac{\mathrm{d}\widehat{\boldsymbol{f}}_{\widehat{\boldsymbol{\theta}}}(\boldsymbol{x})}{\mathrm{d}\widehat{\boldsymbol{\theta}}_L}^\top \end{pmatrix}}_{=:\frac{\mathrm{d}\widehat{\boldsymbol{f}}_{\widehat{\boldsymbol{\theta}}}(\boldsymbol{x})}{\mathrm{d}\widehat{\boldsymbol{\theta}}}^\top \in\mathbb{R}^{\widehat{p}\times n}} \boldsymbol{e}
$$

Preliminaries: Artificial neural networks (ANNs)

Training (learning) and validation: Validation (often in parallel to training) to avoid overfitting

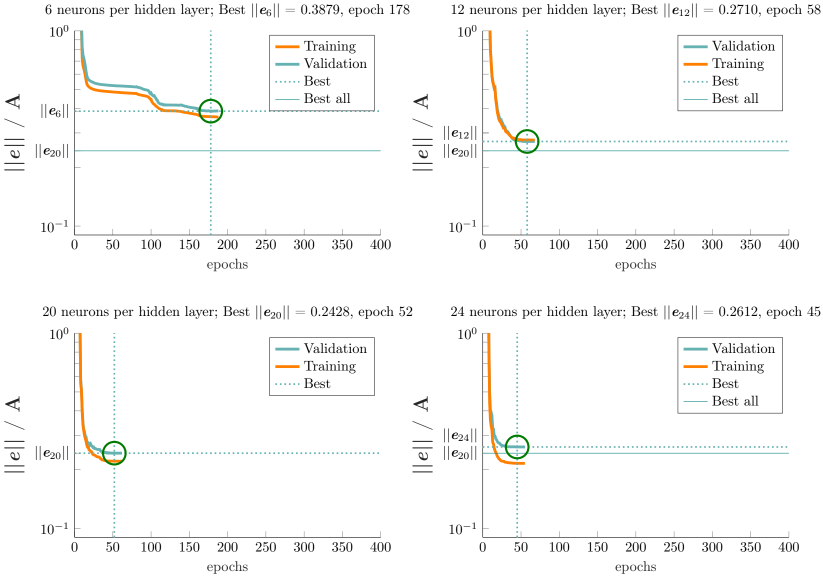

Preliminaries: Artificial neural networks (ANNs)

Key challenges

- **Appropriate data set generation** (and meaningful separation into training and validation set)
- **Appropriate choice of ANN topology** (e.g., number of inputs & outputs, hidden layers and activation functions)
- **Appropriate choice of learning algorithm** (e.g., Gauss-Newton, Levenberg-Marquardt, ADAM)
- **Appropriate integration of HI** (human intelligence, e.g. see distopian or utopian book by Ray Kurzweil)

Outline

3 Example applications

- ANN-based modeling
  - Flux linkage prototype functions (= structered / physics-informed ANNs for flux linkage approximation)
- ANN-based identification
  - Simultaneous identification of inverter and machine nonlinearities
- ANN-based control
  - Optimal feedforward torque control (OFTC) of electrical drives

Example applications

Common applications of AI in electrical drives [24, 166–169] (recap)

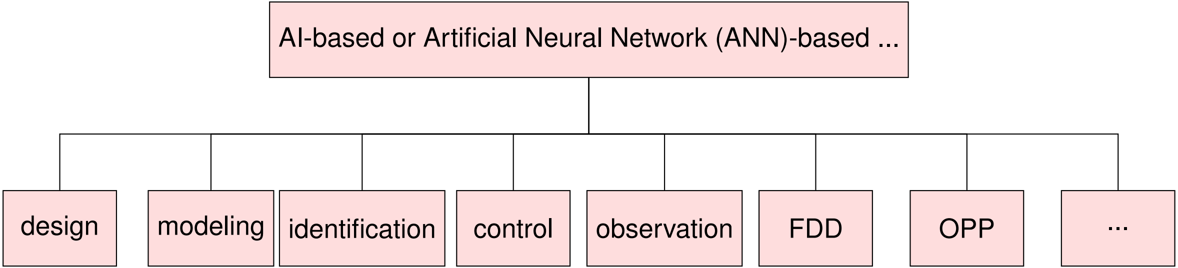

Outline

3 Example applications

- ANN-based modeling
  - Flux linkage prototype functions (= structered / physics-informed ANNs for flux linkage approximation)
- ANN-based identification
  - Simultaneous identification of inverter and machine nonlinearities
- ANN-based control
  - Optimal feedforward torque control (OFTC) of electrical drives

Example applications: ANN-based modeling

Flux linkage prototype functions (= structered / physics-informed ANNs for flux linkage approximation) [25]

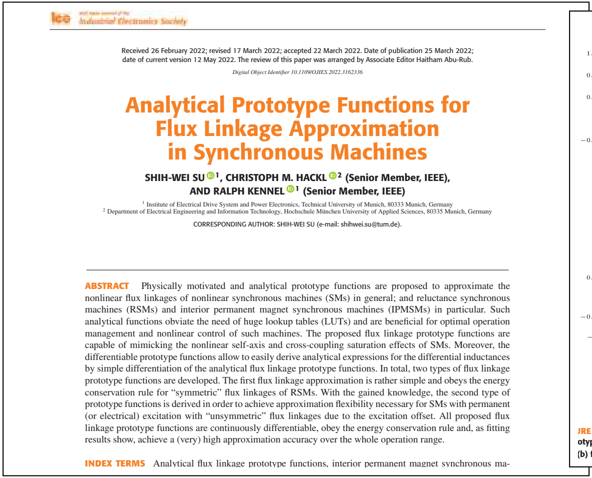

Received 26 February 2022; revised 17 March 2022; accepted 22 March 2022. Date of publication 25 March 2022; date of current version 12 May 2022. The review of this paper was arranged by Associate Editor Haitham Abu-Rub.

Digital Object Identifier 10.1109/OJIES.2022.3162336

Analytical Prototype Functions for Flux Linkage Approximation in Synchronous Machines

SHIH-WEI SU [1], CHRISTOPH M. HACKL [2] (Senior Member, IEEE), AND RALPH KENNEL [1] (Senior Member, IEEE)

[1] Institute of Electrical Drive System and Power Electronics, Technical University of Munich, 80333 Munich, Germany
[2] Department of Electrical Engineering and Information Technology, Hochschule München University of Applied Sciences, 80335 Munich, Germany

CORRESPONDING AUTHOR: SHIH-WEI SU (e-mail: shihwei.su@tum.de).

ABSTRACT Physically motivated and analytical prototype functions are proposed to approximate the nonlinear flux linkages of nonlinear synchronous machines (SMs) in general; and reluctance synchronous machines (RSMs) and interior permanent magnet synchronous machines (IPMSMs) in particular. Such analytical functions obviate the need of huge lookup tables (LUTs) and are beneficial for optimal operation management and nonlinear control of such machines. The proposed flux linkage prototype functions are capable of mimicking the nonlinear self-axis and cross-coupling saturation effects of SMs. Moreover, the differentiable prototype functions allow to easily derive analytical expressions for the differential inductances by simple differentiation of the analytical flux linkage prototype functions. In total, two types of flux linkage prototype functions are developed. The first flux linkage approximation is rather simple and obeys the energy conservation rule for "symmetric" flux linkages of RSMs. With the gained knowledge, the second type of prototype functions is derived in order to achieve approximation flexibility necessary for SMs with permanent (or electrical) excitation with "unsymmetric" flux linkages due to the excitation offset. All proposed flux linkage prototype functions are continuously differentiable, obey the energy conservation rule and, as fitting results show, achieve a (very) high approximation accuracy over the whole operation range.

INDEX TERMS Analytical flux linkage prototype functions, interior permanent magnet synchronous ma-

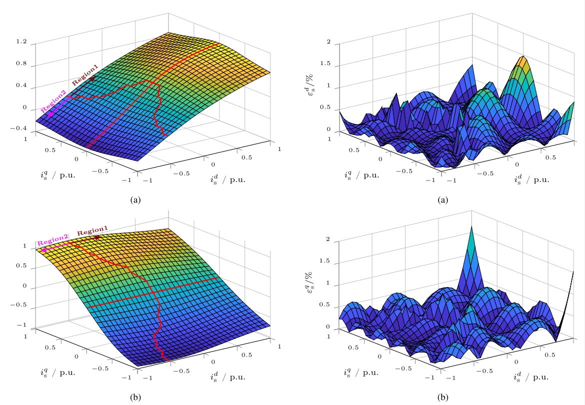

JRE 10. Approximation results of the proposed analytical flux linkage otype functions (40), (41), (46) and (47): (a) fitted d-axis flux linkages (b) fitted q-axis flux linkages $\hat{\psi}_s^q$; zero locus $\mathbb{L}_s^{dq}(L=0)$ [——] is

FIGURE 11. Approximation errors of the proposed analytical flux linkag prototype functions (40), (41), (46) and (47) compared to the real flux maps: (a) normalized d-axis error ε_s^d; (b) normalized q-axis error ε_s^q.

Example applications: ANN-based modeling

Flux linkage prototype functions (= structered / physics-informed ANNs for flux linkage approximation) [25]

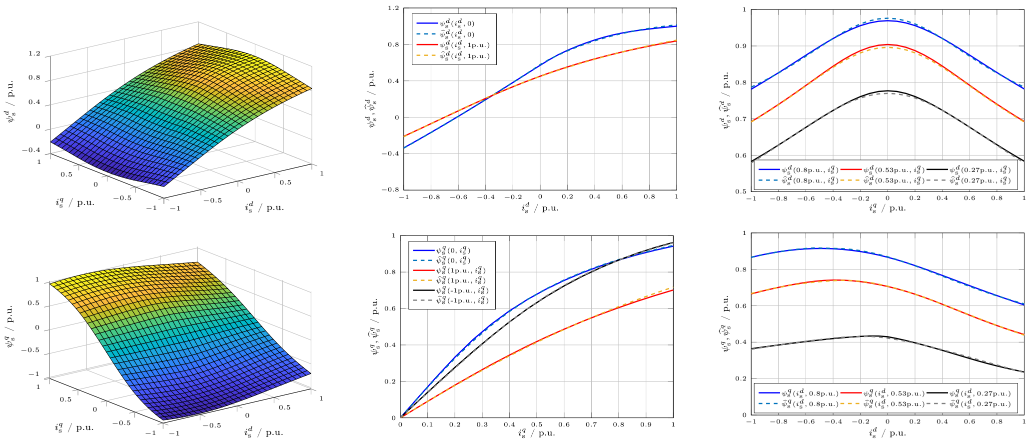

Observation: Flux linkages can be separated into self-axis and cross-axis flux linkage terms:

$$\boldsymbol{\psi}_{\mathrm{s}}^{dq}(\boldsymbol{i}_{\mathrm{s}}^{dq}) = \begin{pmatrix} \psi_{\mathrm{s,self}}^{d}(i_{\mathrm{s}}^{d}) \\ \psi_{\mathrm{s,self}}^{q}(i_{\mathrm{s}}^{q}) \end{pmatrix} - \begin{pmatrix} \psi_{\mathrm{s,cross}}^{d}(i_{\mathrm{s}}^{d}, i_{\mathrm{s}}^{q}) \\ \psi_{\mathrm{s,cross}}^{q}(i_{\mathrm{s}}^{d}, i_{\mathrm{s}}^{q}) \end{pmatrix} \tag{13}$$

Example applications: ANN-based modeling

Flux linkage prototype functions (= structered / physics-informed ANNs for flux linkage approximation) [25]

Further key observations:

To describe the self-axis saturation effects of the flux linkages, the sum of a hyperbolic function and a straight line, i.e.

$$\psi_{\mathrm{s,self}}^{d/q} \propto \tanh(i_{\mathrm{s}}^{d/q}) + i_{\mathrm{s}}^{d/q},$$

seems very well suited for RSMs and also for IPMSMs, whereas to approximate the cross-coupling saturation effects, a (shifted) bell-shaped or Gaussian-like function, i.e.

$$\psi_{\mathrm{s,cross}}^{d/q} \propto -\ln\left(\cosh(i_{\mathrm{s}}^{d/q})\right) \text{ or } \psi_{\mathrm{s,cross}}^{d/q} \propto \exp\left(-(i_{\mathrm{s}}^{d/q})^2\right)$$

seems appropriate for RSMs and for IPMSMs, respectively.

$\Longrightarrow$ Physically motivated, structured function approach for ANN (flux linkage prototype) design!

Example applications: ANN-based modeling

Flux linkage prototype functions (= structered / physics-informed ANNs for flux linkage approximation) [25]

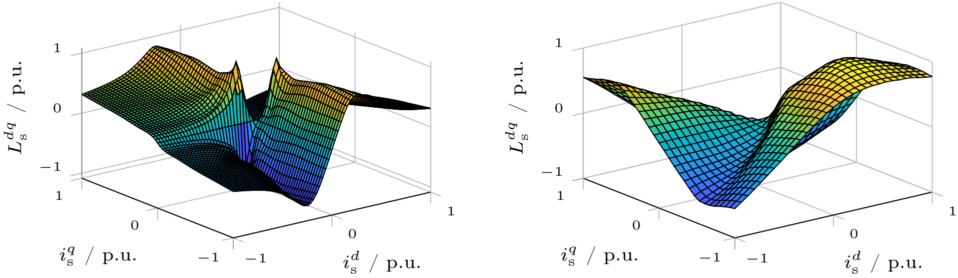

Figure: Differential cross-coupling inductances $L_{\mathrm{s}}^{dq} = L_{\mathrm{s}}^{qd}$ of RSM (left) and IPMSM (right).

Due to **conservation of energy**, we have $\frac{\mathrm{d}}{\mathrm{d}i_{\mathrm{s}}^{q}}\psi_{\mathrm{s}}^{d}(i_{\mathrm{s}}^{d}, i_{\mathrm{s}}^{q}) = \frac{\mathrm{d}}{\mathrm{d}i_{\mathrm{s}}^{d}}\psi_{\mathrm{s}}^{q}(i_{\mathrm{s}}^{d}, i_{\mathrm{s}}^{q}) = -F'(i_{\mathrm{s}}^{d})G'(i_{\mathrm{s}}^{q})$, since

$$\Delta W_{\mathrm{c}}(i_{\mathrm{s}}^{d}, i_{\mathrm{s}}^{q}) = \int \Big(\underbrace{\psi_{\mathrm{s,self}}^{d}(i_{\mathrm{s}}^{d}) - \psi_{\mathrm{s}}^{d}(i_{\mathrm{s}}^{d}, i_{\mathrm{s}}^{q})}_{=\psi_{\mathrm{s,cross}}^{d}(i_{\mathrm{s}}^{d}, i_{\mathrm{s}}^{q}) = F'(i_{\mathrm{s}}^{d})G(i_{\mathrm{s}}^{q})} \Big)\, \mathrm{d}i_{\mathrm{s}}^{d} = \int \Big(\underbrace{\psi_{\mathrm{s,self}}^{q}(i_{\mathrm{s}}^{q}) - \psi_{\mathrm{s}}^{q}(i_{\mathrm{s}}^{d}, i_{\mathrm{s}}^{q})}_{=\psi_{\mathrm{s,cross}}^{q}(i_{\mathrm{s}}^{d}, i_{\mathrm{s}}^{q}) = F(i_{\mathrm{s}}^{d})G'(i_{\mathrm{s}}^{q})} \Big)\, \mathrm{d}i_{\mathrm{s}}^{q} = F(i_{\mathrm{s}}^{d})G(i_{\mathrm{s}}^{q}). \tag{14}$$

Example applications: ANN-based modeling

Flux linkage prototype functions (= structered / physics-informed ANNs for flux linkage approximation) [25]

Analytical flux linkage prototype functions:

$$\widehat{\psi}_{\mathrm{s}}^{d}(i_{\mathrm{s}}^{d}, i_{\mathrm{s}}^{q}) = \widehat{\psi}_{\mathrm{s,self}}^{d}(i_{\mathrm{s}}^{d}) - \widehat{\psi}_{\mathrm{s,cross}}^{d}(i_{\mathrm{s}}^{d}, i_{\mathrm{s}}^{q}) \tag{15}$$

and

$$\widehat{\psi}_{\mathrm{s}}^{q}(i_{\mathrm{s}}^{d}, i_{\mathrm{s}}^{q}) = \widehat{\psi}_{\mathrm{s,self}}^{q}(i_{\mathrm{s}}^{d}) - \widehat{\psi}_{\mathrm{s,cross}}^{q}(i_{\mathrm{s}}^{d}, i_{\mathrm{s}}^{q}) \tag{16}$$

where

$$\widehat{\psi}_{\mathrm{s,cross}}^{d}(i_{\mathrm{s}}^{d}, i_{\mathrm{s}}^{q}) = k_1 F_1'(i_{\mathrm{s}}^{d}) G_1(i_{\mathrm{s}}^{q}) + \cdots + k_{\mathrm{n}} F_{\mathrm{n}}'(i_{\mathrm{s}}^{d}) G_{\mathrm{n}}(i_{\mathrm{s}}^{q}) \tag{17}$$

and

$$\widehat{\psi}_{\mathrm{s,cross}}^{q}(i_{\mathrm{s}}^{d}, i_{\mathrm{s}}^{q}) = k_1 F_1(i_{\mathrm{s}}^{d}) G_1'(i_{\mathrm{s}}^{q}) + \cdots + k_{\mathrm{n}} F_{\mathrm{n}}(i_{\mathrm{s}}^{d}) G_{\mathrm{n}}'(i_{\mathrm{s}}^{q}) \tag{18}$$

with cross-coupling saturation constants $k_1, \cdots, k_{\mathrm{n}}$ and e.g. $F_k(i_{\mathrm{s}}^{d}) = 1 - \mathrm{e}^{-\left(a_k^d (i_{\mathrm{s}}^{d} - b_k^d)\right)^2}$ and $G_k(i_{\mathrm{s}}^{q}) = 1 - \mathrm{e}^{-(a_k^q i_{\mathrm{s}}^{q})^2}$.

The number n of cross-coupling saturation terms in (17) and (18) may be chosen arbitrarily to meet given accuracy requirements. With adequately chosen prototype terms, $n = 3$ or $n = 4$ usually give satisfactory fitting accuracies.

Example applications: ANN-based modeling

Flux linkage prototype functions (= structered / physics-informed ANNs for flux linkage approximation) [25]

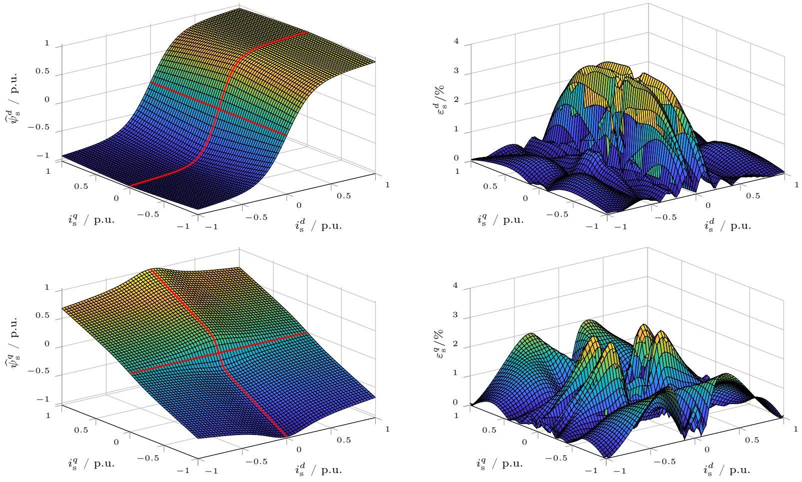

Figure: RSM approximation results of the proposed analytical flux linkage prototype functions: (left) fitted $\widehat{\psi}_s^d(i_s^d, i_s^q)$ and $\widehat{\psi}_s^d(i_s^d, i_s^q)$ (including zero locus $\mathbb{L}_s^{dq}(L=0)$ in red) and (right) relative approximation errors.

Example applications: ANN-based modeling

Flux linkage prototype functions (= structered / physics-informed ANNs for flux linkage approximation) [25]

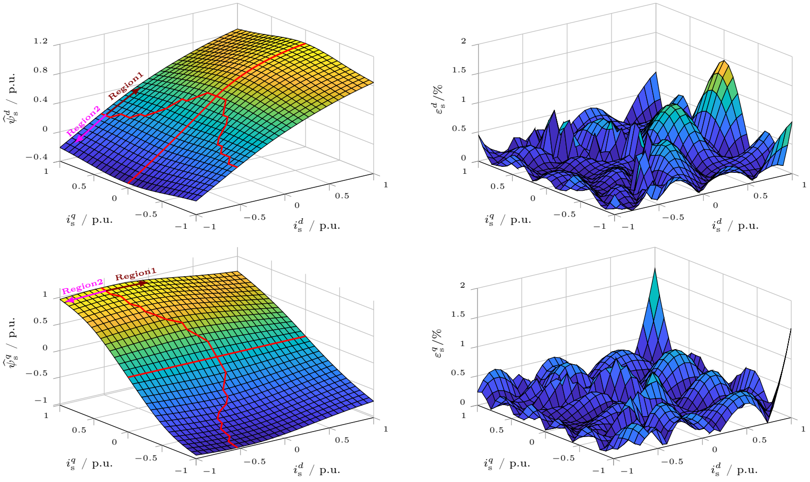

Figure: IPMSM approximation results of the proposed analytical flux linkage prototype functions: (left) fitted $\widehat{\psi}_{\mathrm{s}}^{d}(i_{\mathrm{s}}^{d}, i_{\mathrm{s}}^{q})$ and $\widehat{\psi}_{\mathrm{s}}^{d}(i_{\mathrm{s}}^{d}, i_{\mathrm{s}}^{q})$ (including zero locus $\mathbb{L}_{\mathrm{s}}^{dq}(L=0)$ in red) and (right) relative approximation errors.

Outline

Example applications: ANN-based identification

Simultaneous identification of inverter and machine nonlinearities [138]

IEEE TRANSACTIONS ON ENERGY CONVERSION, VOL. 38, NO. 3, SEPTEMBER 2023 1767

Simultaneous Identification of Inverter and Machine Nonlinearities for Self-Commissioning of Electrical Synchronous Machine Drives

Simon Wiedemann and Christoph Michael Hackl, *Senior Member, IEEE*

Abstract—**The proposed identification method allows for a simultaneous estimation of nonlinear output voltage deviations in voltage source inverters (VSIs) and nonlinear synchronous machine models. Based on the identified characteristics with the help of physically inspired structured artificial neural networks (ANNs), an efficient tuning of the current control system can be performed and the nonlinear voltage deviations caused by parasitic effects and dead-time distortions can be accurately compensated for. The identification is performed without position sensor while the rotor is mechanically locked by utilising measured phase currents and reference machine voltages only. Experiments for an interior permanent magnet synchronous machine (IPMSM) and a reluctance synchronous machine (RSM) show that the proposed method is capable of identifying the current dependent self-axis and cross-axis flux linkages, differential inductances and the nonlinear VSI voltage deviations as well as the phase resistance at the same time. The proposed method is fast and generic. Besides the rated machine current, voltage and frequency, no prior system knowledge is required making it applicable for the self-commissioning of any electrical synchronous machine drive.**

Index Terms—**Identification, self-commissioning, auto-tuning, synchronous machine, inverter dead-time, machine characterisation, flux linkage map, machine model, artificial neural network, encoderless.**

NOTATION

$\mathbb{N}, \mathbb{R}$: natural, real numbers; $\boldsymbol{x} := (x_1, \ldots, x_n)^\top \in \mathbb{R}[n]$: col-

I. INTRODUCTION

MODERN control methods and observer architectures of electrical machines rely mostly on accurate information of drive characteristics. Identified parameters of the linear machine model such as the phase resistances and inductances can be utilised to tune the current controllers [1], [2], [3] or observers and to compute the optimal reference currents for an energy efficient operation [2], [4]. This tuning can be further improved by the identification and utilisation of nonlinear flux linkage maps usually expressed in the synchronously rotating (d, q)-reference frame [2], [4], [5], [6], [7], [8] which allow to compute the differential inductances (in the following, the superscript d or q stands for the d- or q-axis, resp.). The automatic identification and tuning of the machine drive can be considered as self-commissioning/auto-tuning and is usually performed before machine operation via offline identification [1], [2], [9].

Self-commissioning algorithms heavily decrease the time required to characterise and tune an electrical machine drive compared to a manual process which, due to a lack of expertise and time of the control engineers, might lead to imprecise results and poor control dynamics [2] as well as an energy inefficient operation [9]. The importance of an automatic commissioning becomes obvious if one considers that around 53 % of the globally generated energy is consumed by electrical machines [10]. Despite several improvements on energy efficient

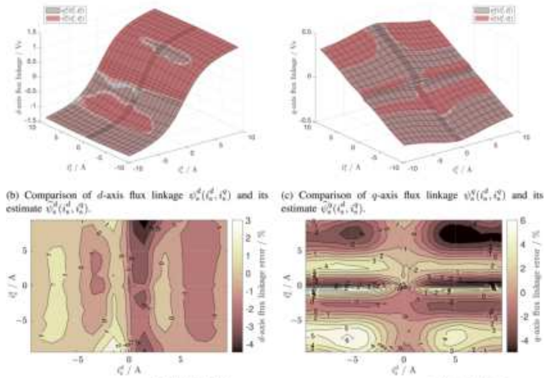

(b) Comparison of d-axis flux linkage $\psi_s^d(i_s^d, i_s^q)$ and its estimate $\widehat{\psi}_s^d(i_s^d, i_s^q)$.

(c) Comparison of q-axis flux linkage $\psi_s^q(i_s^d, i_s^q)$ and its estimate $\widehat{\psi}_s^q(i_s^d, i_s^q)$.

(d) Relative d-flux linkage error $\frac{\psi_s^d(i_s^d,i_s^q)-\widehat{\psi}_s^d(i_s^d,i_s^q)}{\psi_{s,\max}}$.

(e) Relative q-flux linkage error $\frac{\psi_s^q(i_s^d,i_s^q)-\widehat{\psi}_s^q(i_s^d,i_s^q)}{\psi_{s,\max}}$.

ig. 9. **RSM identification results:** (a) Time series; (b) & (c) flux linkages; (e) & (f) relative flux linkage errors.

ı significantly increased model complexity as for which it is ... -4% to 3% for $\widehat{\psi}_s^d(i_s^d, i_s^q)$ and -4% to 6% for $\widehat{\psi}_s^q(i_s^d, i_s^q)$. Fig. 1

Example applications: ANN-based identification

Simultaneous identification of inverter and machine nonlinearities [138]

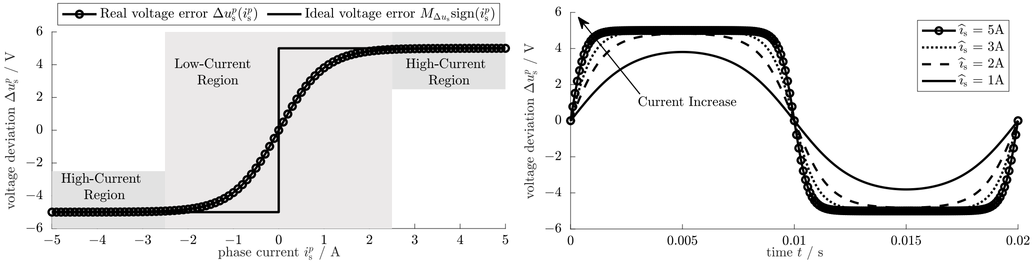

Figure: Ideal vs. real voltage deviation over i_s^p (left); real voltage deviation $\Delta u_s^p(i_s^p)$ over one period of a sinusoidal phase current i_s^p with different amplitudes $\widehat{\imath}_s$ (right).

Inverter nonlinearities (also depending on dc-link voltage):

$$\forall\, p \in \{a, b, c\}: \qquad u_s^p = u_{s,\mathrm{ref}}^p - \Delta u_s^p(M_{\Delta u_s}, i_s^p, \ldots). \tag{19}$$

Example applications: ANN-based identification

Simultaneous identification of inverter and machine nonlinearities [138]

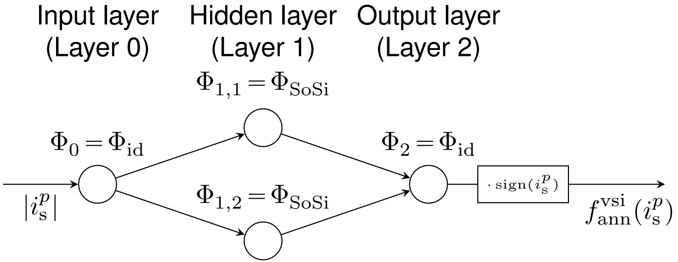

Figure: ANN for approximation of VSI voltage deviation Δu_{s}^p of phase $p \in \{a, b, c\}$ by $\Delta \widehat{u}_{\mathrm{s}}^p := f_{\mathrm{ann}}^{\mathrm{vsi}}(i_{\mathrm{s}}^p)$.

Resulting ANN structure for VSI identification:

$$\begin{aligned}\Delta \widehat{u}_{\mathrm{s}}^p(i_{\mathrm{s}}^p) &:= f_{\mathrm{ann}}^{\mathrm{vsi}}(i_{\mathrm{s}}^p) \\ &= \left(\frac{w_{2,1}^{\mathrm{vsi}}\left(w_{1,1}^{\mathrm{vsi}}|i_{\mathrm{s}}^p| + b_{1,1}^{\mathrm{vsi}}\right)}{1 + |w_{1,1}^{\mathrm{vsi}}|i_{\mathrm{s}}^p| + b_{1,1}^{\mathrm{vsi}}|} + \frac{w_{2,2}^{\mathrm{vsi}}\left(w_{1,2}^{\mathrm{vsi}}|i_{\mathrm{s}}^p| + b_{1,2}^{\mathrm{vsi}}\right)}{1 + |w_{1,2}^{\mathrm{vsi}}|i_{\mathrm{s}}^p| + b_{1,2}^{\mathrm{vsi}}|} \right) \mathrm{sign}(i_{\mathrm{s}}^p) \end{aligned} \tag{20}$$

Example applications: ANN-based identification

Simultaneous identification of inverter and machine nonlinearities [138]

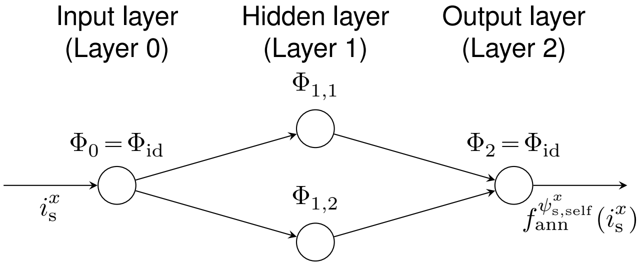

Figure: Approximating ANN for self-axis flux linkage $\psi_{\mathrm{s,self}}^x(i_{\mathrm{s}}^x)$ of axis $x \in \{d, q\}$ by $\widehat{\psi}_{\mathrm{s,self}}^x(i_{\mathrm{s}}^x) := f_{\mathrm{ann}}^{\psi_{\mathrm{s,self}}^x}(i_{\mathrm{s}}^x)$.

Resulting physics-informed ANN topology for self-axis flux linkage identification:

$$\widehat{\psi}_{\mathrm{s,self}}^x(i_{\mathrm{s}}^x) = w_{2,1}^{x,\mathrm{self}} \frac{1-\exp\left(-2(w_{1,1}^{x,\mathrm{self}} i_{\mathrm{s}}^x + b_{1,1}^{x,\mathrm{self}})\right)}{1+\exp\left(-2(w_{1,1}^{x,\mathrm{self}} i_{\mathrm{s}}^x + b_{1,1}^{x,\mathrm{self}})\right)} + w_{2,2}^{x,\mathrm{self}} \frac{1-\exp\left(-2(w_{1,2}^{x,\mathrm{self}} i_{\mathrm{s}}^x + b_{1,2}^{x,\mathrm{self}})\right)}{1+\exp\left(-2(w_{1,2}^{x,\mathrm{self}} i_{\mathrm{s}}^x + b_{1,2}^{x,\mathrm{self}})\right)} + b_2^{x,\mathrm{self}} \tag{21}$$

or (for rather linear machines)

$$\widehat{\psi}_{\mathrm{s,self}}^x(i_{\mathrm{s}}^x) := w_{2,1}^{x,\mathrm{self}} i_{\mathrm{s}}^x - w_{2,2}^{x,\mathrm{self}} \ln\left(1 + \exp(-i_{\mathrm{s}}^x)\right) + b_2^{x,\mathrm{self}} \tag{22}$$

Example applications: ANN-based identification

Simultaneous identification of inverter and machine nonlinearities [138]

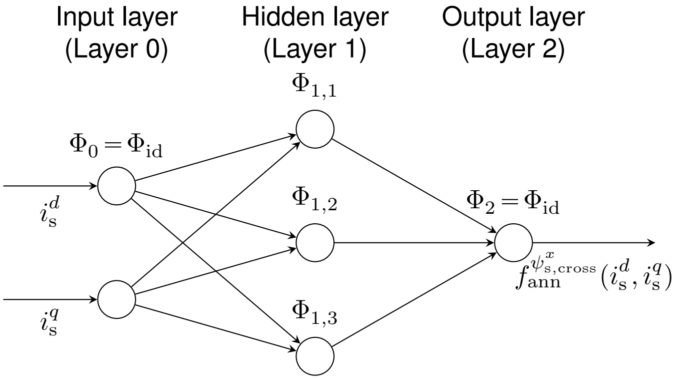

Figure: Approximating ANN for cross-axis flux linkage $\psi_{\mathrm{s,cross}}^{x}(i_{\mathrm{s}}^{d}, i_{\mathrm{s}}^{q})$ of axis $x \in \{d, q\}$ by $\widehat{\psi}_{\mathrm{s,cross}}^{x}(i_{\mathrm{s}}^{d}, i_{\mathrm{s}}^{q}) := f_{\mathrm{ann}}^{\psi_{\mathrm{s,cross}}^{x}}(i_{\mathrm{s}}^{d}, i_{\mathrm{s}}^{q})$.

Example applications: ANN-based identification

Simultaneous identification of inverter and machine nonlinearities [138]

Resulting physics-informed ANN topology for cross-axis flux linkage identification for

$$
\text{RSMs:}\ \begin{cases}
\widehat{\psi}^{d}_{\mathrm{s,cross}}(i^d_{\mathrm{s}}, i^q_{\mathrm{s}}) &= 2w^{\mathrm{cross}}_{2,1}(w^{d,\mathrm{cross}}_{1,1})^2 i^d_{\mathrm{s}} \exp\Big(-(w^{d,\mathrm{cross}}_{1,1} i^d_{\mathrm{s}})^2\Big)\Big(1-\exp\Big(-(w^{q,\mathrm{cross}}_{1,1} i^q_{\mathrm{s}})^2\Big)\Big) \\
&\quad +2w^{\mathrm{cross}}_{2,2}(w^{d,\mathrm{cross}}_{1,2})^2 i^d_{\mathrm{s}} \exp\Big(-(w^{d,\mathrm{cross}}_{1,2} i^d_{\mathrm{s}})^2\Big)\Big(1-\exp\Big(-(w^{q,\mathrm{cross}}_{1,2} i^q_{\mathrm{s}})^2\Big)\Big) \\
\widehat{\psi}^{q}_{\mathrm{s,cross}}(i^d_{\mathrm{s}}, i^q_{\mathrm{s}}) &= 2w^{\mathrm{cross}}_{2,1}(w^{q,\mathrm{cross}}_{1,1})^2 i^q_{\mathrm{s}} \exp\Big(-(w^{q,\mathrm{cross}}_{1,1} i^q_{\mathrm{s}})^2\Big)\Big(1-\exp\Big(-(w^{d,\mathrm{cross}}_{1,1} i^d_{\mathrm{s}})^2\Big)\Big) \\
&\quad +2w^{\mathrm{cross}}_{2,2}(w^{q,\mathrm{cross}}_{1,2})^2 i^q_{\mathrm{s}} \exp\Big(-(w^{q,\mathrm{cross}}_{1,2} i^q_{\mathrm{s}})^2\Big)\Big(1-\exp\Big(-(w^{d,\mathrm{cross}}_{1,2} i^d_{\mathrm{s}})^2\Big)\Big).
\end{cases} \tag{23}
$$

Example applications: ANN-based identification

Simultaneous identification of inverter and machine nonlinearities [138]

Resulting physics-informed ANN topology for cross-axis flux linkage identification for

$$
\text{IPMSMs: } \left\{
\begin{aligned}
\widehat{\psi}^{d}_{\mathrm{s,cross}}(i^d_{\mathrm{s}}, i^q_{\mathrm{s}}) \;=\;& w^{\mathrm{cross}}_{2,1}\Big(w^{d,\mathrm{cross}}_{1,1,1} + 2w^{d,\mathrm{cross}}_{1,1,2}\, i^d_{\mathrm{s}} + \tfrac{w^{d,\mathrm{cross}}_{1,1,3}}{1+\exp(-(i^d_{\mathrm{s}}+b^{d,\mathrm{cross}}_{1,1}))}\Big)\cdot \\
& \Big(w^{q,\mathrm{cross}}_{1,1,1}\, i^q_{\mathrm{s}} + w^{q,\mathrm{cross}}_{1,1,2}\,(i^q_{\mathrm{s}})^2 + w^{q,\mathrm{cross}}_{1,1,3}\ln\big(\exp(i^q_{\mathrm{s}} + b^{q,\mathrm{cross}}_{1,1}) + 1\big)\Big) \\
& + w^{\mathrm{cross}}_{2,2}\Big(w^{d,\mathrm{cross}}_{1,2,1} + 2w^{d,\mathrm{cross}}_{1,2,2}\, i^d_{\mathrm{s}} + \tfrac{w^{d,\mathrm{cross}}_{1,2,3}}{1+\exp(-(i^d_{\mathrm{s}}+b^{d,\mathrm{cross}}_{1,2}))}\Big)\cdot \\
& \Big(w^{q,\mathrm{cross}}_{1,2,1}\, i^q_{\mathrm{s}} + w^{q,\mathrm{cross}}_{1,2,2}\,(i^q_{\mathrm{s}})^2 + w^{q,\mathrm{cross}}_{1,2,3}\ln\big(\exp(i^q_{\mathrm{s}} + b^{q,\mathrm{cross}}_{1,2}) + 1\big)\Big) \\
& + w^{\mathrm{cross}}_{2,3}\Big(w^{d,\mathrm{cross}}_{1,3,1} + 2w^{d,\mathrm{cross}}_{1,3,2}\, i^d_{\mathrm{s}} + \tfrac{w^{d,\mathrm{cross}}_{1,3,3}}{1+\exp(-(i^d_{\mathrm{s}}+b^{d,\mathrm{cross}}_{1,3}))}\Big)\cdot \\
& \Big(w^{q,\mathrm{cross}}_{1,3,1}\, i^q_{\mathrm{s}} + w^{q,\mathrm{cross}}_{1,3,2}\,(i^q_{\mathrm{s}})^2 + w^{q,\mathrm{cross}}_{1,3,3}\ln\big(\exp(i^q_{\mathrm{s}} + b^{q,\mathrm{cross}}_{1,3}) + 1\big)\Big) \\
\widehat{\psi}^{q}_{\mathrm{s,cross}}(i^d_{\mathrm{s}}, i^q_{\mathrm{s}}) \;=\;& w^{\mathrm{cross}}_{2,1}\Big(w^{q,\mathrm{cross}}_{1,1,1} + 2w^{q,\mathrm{cross}}_{1,1,2}\, i^q_{\mathrm{s}} + \tfrac{w^{q,\mathrm{cross}}_{1,1,3}}{1+\exp(-(i^q_{\mathrm{s}}+b^{q,\mathrm{cross}}_{1,1}))}\Big)\cdot \\
& \Big(w^{d,\mathrm{cross}}_{1,1,1}\, i^d_{\mathrm{s}} + w^{d,\mathrm{cross}}_{1,1,2}\,(i^d_{\mathrm{s}})^2 + w^{d,\mathrm{cross}}_{1,1,3}\ln\big(\exp(i^d_{\mathrm{s}} + b^{d,\mathrm{cross}}_{1,1}) + 1\big)\Big) \\
& + w^{\mathrm{cross}}_{2,2}\Big(w^{q,\mathrm{cross}}_{1,2,1} + 2w^{q,\mathrm{cross}}_{1,2,2}\, i^q_{\mathrm{s}} + \tfrac{w^{q,\mathrm{cross}}_{1,2,3}}{1+\exp(-(i^q_{\mathrm{s}}+b^{q,\mathrm{cross}}_{1,2}))}\Big)\cdot \\
& \Big(w^{d,\mathrm{cross}}_{1,2,1}\, i^d_{\mathrm{s}} + w^{d,\mathrm{cross}}_{1,2,2}\,(i^d_{\mathrm{s}})^2 + w^{d,\mathrm{cross}}_{1,2,3}\ln\big(\exp(i^d_{\mathrm{s}} + b^{d,\mathrm{cross}}_{1,2}) + 1\big)\Big) \\
& + w^{\mathrm{cross}}_{2,3}\Big(w^{q,\mathrm{cross}}_{1,3,1} + 2w^{q,\mathrm{cross}}_{1,3,2}\, i^q_{\mathrm{s}} + \tfrac{w^{q,\mathrm{cross}}_{1,3,3}}{1+\exp(-(i^q_{\mathrm{s}}+b^{d,\mathrm{cross}}_{1,3}))}\Big)\cdot \\
& \Big(w^{d,\mathrm{cross}}_{1,3,1}\, i^d_{\mathrm{s}} + w^{d,\mathrm{cross}}_{1,3,2}\,(i^d_{\mathrm{s}})^2 + w^{d,\mathrm{cross}}_{1,3,3}\ln\big(\exp(i^d_{\mathrm{s}} + b^{d,\mathrm{cross}}_{1,3}) + 1\big)\Big).
\end{aligned}
\right\} \tag{24}
$$

Example applications: ANN-based identification

Simultaneous identification of inverter and machine nonlinearities [138]

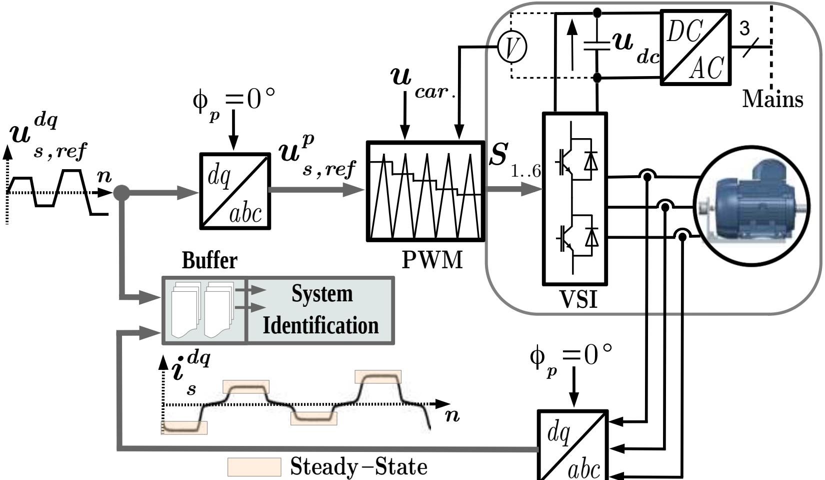

Figure: Simplified block diagram of the excitation and identification process.

Example applications: ANN-based identification

Simultaneous identification of inverter and machine nonlinearities [138]

Table: Considered machines and key data.

Machine Type	 **M1: IPMSM**	 **M2: RSM**
Manufacturer	EMP	Stellenbosch
Designation	Prototype	Prototype
Rated Phase Current I_{R}	4.07 A$_{\mathrm{rms}}$	3.54 A$_{\mathrm{rms}}$
Rated Torque $m_{\mathrm{m,R}}$	2.06 Nm	9.60 Nm
Poles	$8\ (n_{\mathrm{p}} = 4)$	$4\ (n_{\mathrm{p}} = 2)$
Rated Speed $n_{\mathrm{m,R}}$	$6\,000$ rpm	$1\,500$ rpm

Example applications: ANN-based identification

Simultaneous identification of inverter and machine nonlinearities [138]

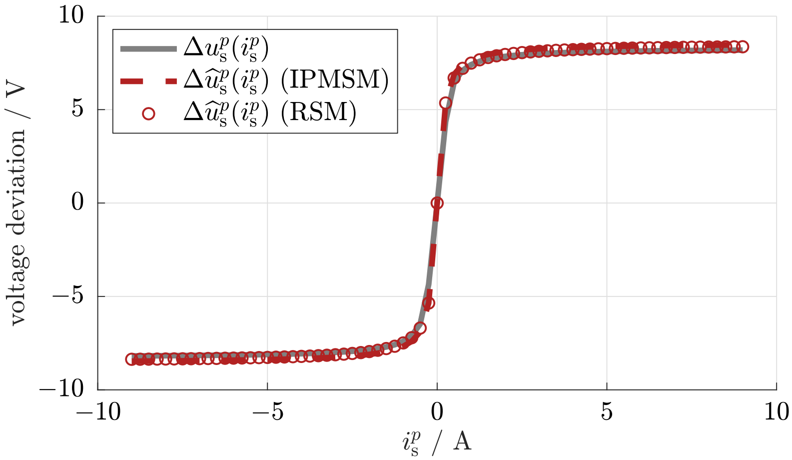

Figure: **IPMSM and RSM identification results:** Comparison of VSI voltage deviations $\Delta u_s^p(i_s^p)$ and their estimates $\Delta \widehat{u}_s^p(i_s^p)$ (d and q axis give very similar results).

Example applications: ANN-based identification

Simultaneous identification of inverter and machine nonlinearities [138]

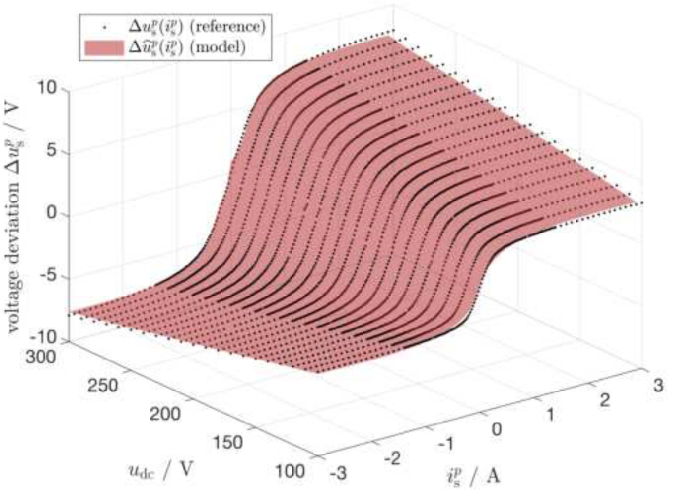

Remark 4 (Dependency on dc-link voltage)

To consider a varying u_{dc}, the ANN structure in (20) has to be extended by replacing the terms $x_1 := w_{1,1}^{vsi}|i_s^p| + b_{1,1}^{vsi}$ and $x_2 := w_{1,2}^{vsi}|i_s^p| + b_{1,2}^{vsi}$ by $x_1 := w_{1,1}^{vsi}|i_s^p| + w_{1,3}^{vsi}u_{dc} + b_{1,1}^{vsi}$ and $x_2 := w_{1,2}^{vsi}|i_s^p| + w_{1,4}^{vsi}u_{dc} + b_{1,2}^{vsi}$, respectively. Then, the VSI-ANN depends not only on the phase current i_s^p but also on the dc-link voltage u_{dc} and has two more weights $w_{1,3}^{vsi}$ and $w_{1,4}^{vsi}$.

Example applications: ANN-based identification

Simultaneous identification of inverter and machine nonlinearities [138]

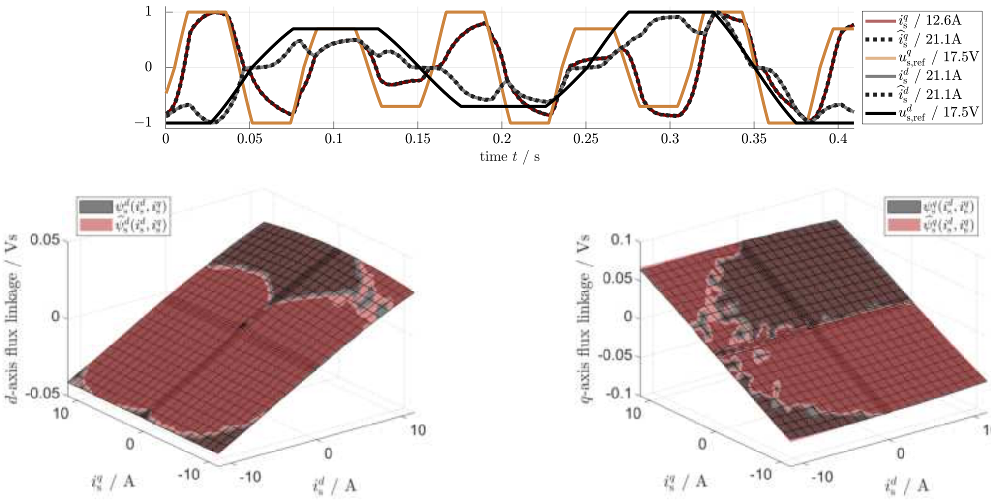

Figure: **IPMSM identification results:** Time series (top) and flux linkage maps (bottom)

Example applications: ANN-based identification

Simultaneous identification of inverter and machine nonlinearities [138]

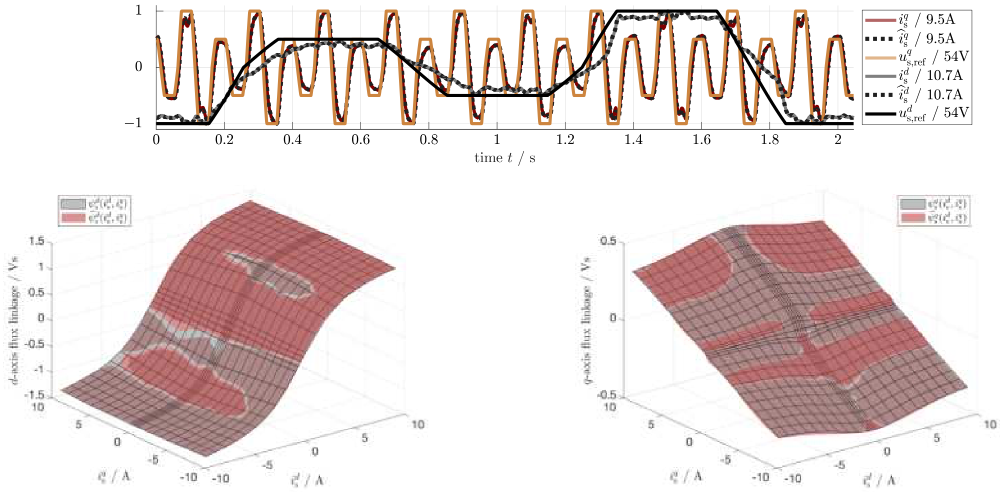

Figure: **RSM identification results:** Time series (top) and flux linkage maps (bottom)

Outline

3 Example applications

- ANN-based modeling
  - Flux linkage prototype functions (= structered / physics-informed ANNs for flux linkage approximation)
- ANN-based identification
  - Simultaneous identification of inverter and machine nonlinearities
- ANN-based control
  - Optimal feedforward torque control (OFTC) of electrical drives

Example applications: ANN-based control

Optimal feedforward torque control (OFTC) of electrical drives (see, e.g., [24, 173, 174]): Problem statement

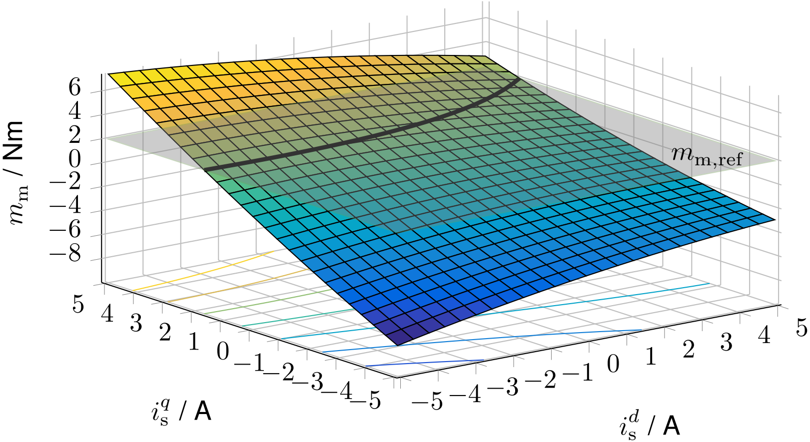

$$m_{\mathrm{m,ref}} \overset{!}{=} m_{\mathrm{m}}\left(\boldsymbol{i}_{\mathrm{s}}^{dq}\right) = \frac{2n_{\mathrm{p}}}{3\kappa^2}\left[\widetilde{\psi}_{\mathrm{pm}} i_{\mathrm{s}}^{q} + \left(\widetilde{L}_{\mathrm{s}}^{d} - \widetilde{L}_{\mathrm{s}}^{q}\right) i_{\mathrm{s}}^{d} i_{\mathrm{s}}^{q} + \widetilde{L}_{\mathrm{s,m}}\left((i_{\mathrm{s}}^{q})^2 - (i_{\mathrm{s}}^{d})^2\right)\right] \Longrightarrow \boxed{\boldsymbol{i}_{\mathrm{s,ref}}^{dq} := (?, ?)^\top}$$

Example applications: ANN-based control

Optimal feedforward torque control (OFTC) of electrical drives (see, e.g., [24, 173, 174]): Problem similar for all machines!

Nonlinear IPMSM (3.9 kW@5 500 rpm)

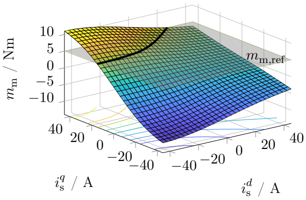

Nonlinear IM (3 kW@1 445 rpm)

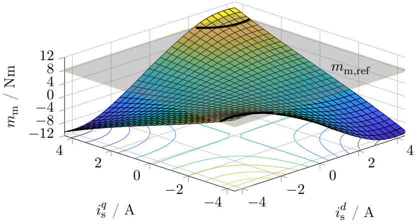

Nonlinear DFIM (10 kW@1 500 rpm)

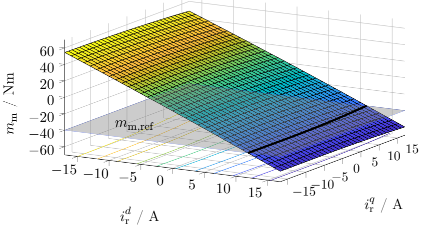

Nonlinear RSM (9.6 kW@1 500 rpm)

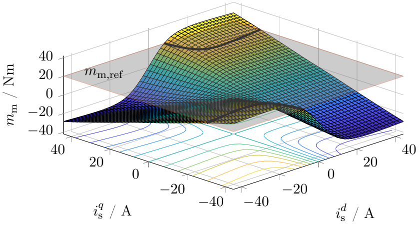

Example applications: ANN-based control

Optimal feedforward torque control (OFTC) of electrical drives (see, e.g., [24, 173, 174]): ANN-based OFTC of EESMs

Artificial neural network based optimal feedforward torque control of electrically excited synchronous machines

1st Niklas Monzen and 2nd Christoph M. Hackl
Laboratory for Mechatronic and Renewable Energy Systems (LMRES)
HM Munich University of Applied Sciences
Munich, Germany
{niklas.monzen, christoph.hackl}@hm.edu

***Abstract*—An Artificial Neural Network (ANN) based Optimal Feedforward Torque Control (OFTC) strategy for electrically excited synchronous machines (EESMs) is proposed. After design, data set creation, training and validation of the ANN, the analytical computation of the optimal stator and exciter currents is achieved which allows to minimize copper and iron losses and to produce the desired (or maximally feasible) machine torque. Voltage and currents constraints of stator and exciter are considered as well. In contrast to conventional OFTC, the proposed ANN-based OFTC strategy does not require iterations nor a decision tree to find the optimal current triple while machine nonlinearities, magnetic cross-coupling, saturation and speed-dependent iron losses are taken into account. In addition, the proposed ANN design procedure allows to consider *measurable* OFTC goals and computational resources that ensures a real-time capable implementation. Comprehensive simulation results for a real and nonlinear EESM clearly show these benefits by comparing the proposed ANN-based OFTC with results of a nonlinear optimization problem (NLP) solver (which cannot be used in real-time).**

***Index Terms*—Artificial neural network (ANN), copper & iron losses, efficiency, electrically excited synchronous machine (EESM), machine learning, nonlinear machine model, optimal feedforward torque control (OFTC), optimal reference current computation, optimization.**

a unified theory was presented that covers different operating strategies such as Maximum-Torque-per-Ampere (MTPA; or Maximum-Torque-per-Current (MTPC)), Field Weakening (FW), Maximum Current (MC) and Maximum-Torque-per-Voltage (MTPV) and allows to compute the optimal stator reference currents for RSM and PMSM analytically without simplifying assumptions on flux linkage nonlinearities or stator resistances. However, iron losses were neglected. This has been overcome by the extended analytical approach presented in [17, 24]. But EESMs, with additional exciter current, are not covered.

In [28–30] numerical identification and search algorithms are proposed as *offline* OFTC approaches for EESM that are not suitable for a real-time implementation.

In [31], the MTPA problem for stator and exciter currents is solved by the use of a Lagrangian. However, electromagnetic cross-coupling and iron losses are not considered. Furthermore, the reference currents are computed offline and stored in look-up tables (LUTs) due to the computationally expensive solution of the MTPA problem.

In [32–36] online OFTC approaches are presented that are

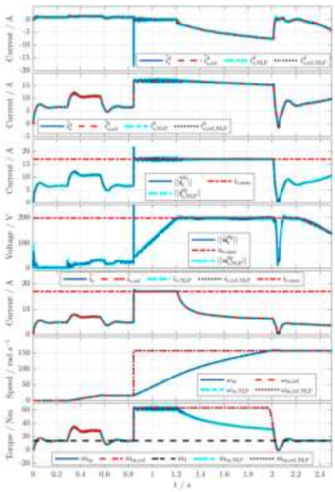

Figure 6: Implementation results for the proposed ANN-based OFTC for a real, nonlinear EESM (from top to bottom): Time series of stator currents, current magnitude, voltage norm/limit, exciter current, angular velocity and torque.

Example applications: ANN-based control

Optimal feedforward torque control (OFTC) of electrical drives (see, e.g., [24, 173, 174]): ANN-based OFTC of EESMs

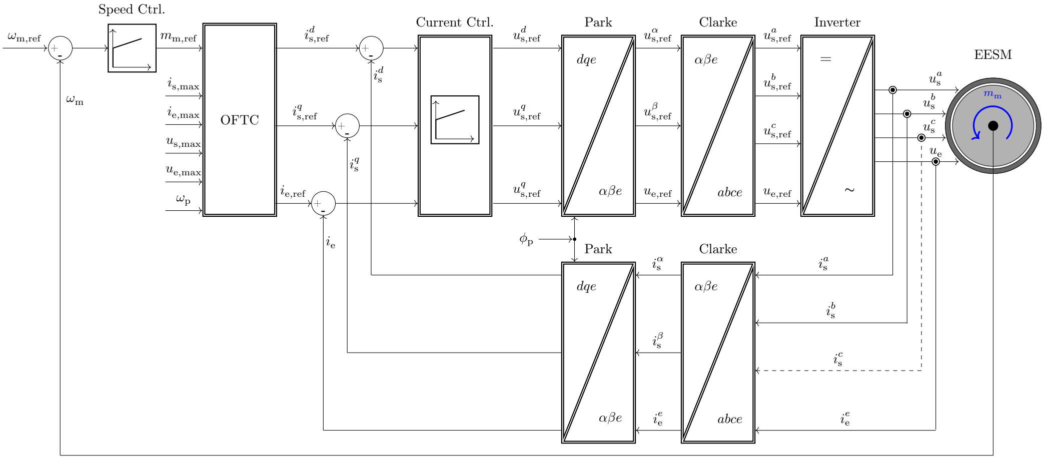

Example applications: ANN-based control

Optimal feedforward torque control (OFTC) of electrical drives (see, e.g., [24, 173, 174]): ANN-based OFTC of EESMs

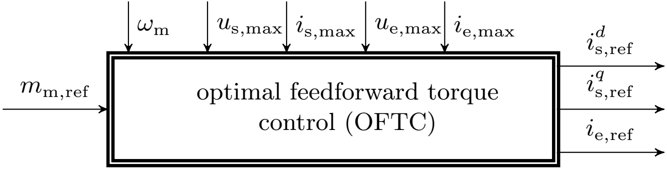

Equivalent circuit:

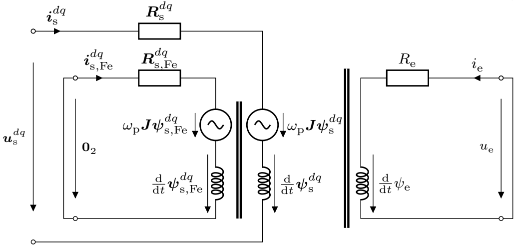

Nonlinear optimization problem:

$$
\begin{aligned}
\boldsymbol{i}^{dqe}_{\mathrm{s,e,ref}}[k] = \underset{\boldsymbol{i}^{dqe}_{\mathrm{s,e}}[k]}{\arg\min}\quad & p_{\mathrm{L}}\big(\boldsymbol{i}^{dqe}_{\mathrm{s,e}}[k]\big) \\
\text{s.t.} \qquad & \big\|\boldsymbol{u}^{dq}_{\mathrm{s}}\big(\boldsymbol{i}^{dqe}_{\mathrm{s,e}}[k]\big)\big\| \leqslant u_{\mathrm{s,max}}[k], \\
& \big\|\boldsymbol{i}^{dq}_{\mathrm{s}}[k]\big\| \leqslant i_{\mathrm{s,max}}[k], \\
& \big|u_{\mathrm{e}}\big(\boldsymbol{i}^{dqe}_{\mathrm{s,e}}[k]\big)\big| \leqslant u_{\mathrm{e,max}}[k], \\
& \big|i_{\mathrm{e}}[k]\big| \leqslant i_{\mathrm{e,max}}[k], \\
& m_{\mathrm{m}}\big(\boldsymbol{i}^{dqe}_{\mathrm{s,e}}[k]\big) = \overline{m}_{\mathrm{m,ref}}\big(\boldsymbol{i}^{dqe}_{\mathrm{s,e}}[k]\big)
\end{aligned}
\qquad (25)
$$

Example applications: ANN-based control

Optimal feedforward torque control (OFTC) of electrical drives (see, e.g., [24, 173, 174]): ANN-based OFTC of EESMs

What is the best ANN topology (number of hidden layers, neurons, activation functions, etc.)?

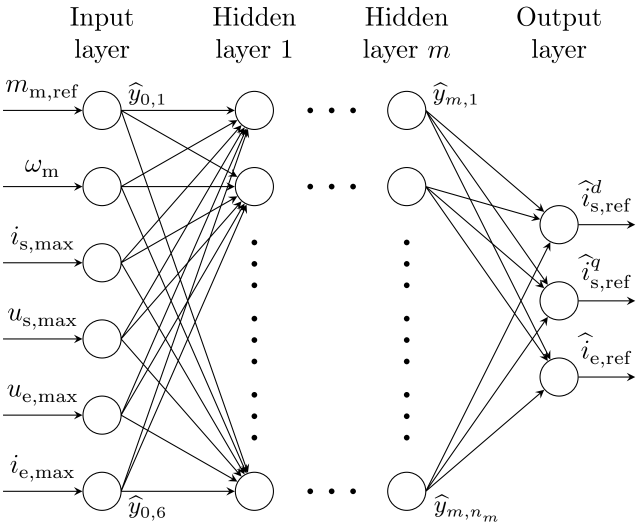

Example applications: ANN-based control

Optimal feedforward torque control (OFTC) of electrical drives (see, e.g., [24, 173, 174]): ANN-based OFTC of EESMs

Multi-objective optimization considering additionally physical constraints, such that

$$\left.\begin{aligned}
e_{\mathrm{u_s}} &= \tfrac{1}{K}\textstyle\sum_{k=1}^{K} \max\left(0, \|\widehat{\boldsymbol{u}}_{\mathrm{s}}^{dq}[k]\| - u_{\mathrm{s,max}}[k]\right)^2, \\
e_{\mathrm{i_s}} &= \tfrac{1}{K}\textstyle\sum_{k=1}^{K} \max\left(0, \|\widehat{\boldsymbol{i}}_{\mathrm{s,ref}}^{dq}[k]\| - i_{\mathrm{s,max}}[k]\right)^2, \\
e_{\mathrm{u_e}} &= \tfrac{1}{K}\textstyle\sum_{k=1}^{K} \max\left(0, |\widehat{u}_{\mathrm{e}}[k]| - u_{\mathrm{e,max}}[k]\right)^2, \\
e_{\mathrm{i_e}} &= \tfrac{1}{K}\textstyle\sum_{k=1}^{K} \max\left(0, |\widehat{i}_{\mathrm{e,ref}}[k]| - i_{\mathrm{e,max}}[k]\right)^2, \\
e_{\mathrm{m}} &= \tfrac{1}{K}\textstyle\sum_{k=1}^{K} \left(\widehat{m}_{\mathrm{m}}[k] - \overline{m}_{\mathrm{m,ref}}[k]\right)^2, \\
e_{\mathrm{L}} &= \tfrac{1}{K}\textstyle\sum_{k=1}^{K} \left(\widehat{p}_{\mathrm{L}}[k] - p_{\mathrm{L}}[k]\right)^2
\end{aligned}\right\} \tag{26}$$

in order to find **Pareto optimal ANN architecture** as trade-off between the three OFTC criteria:

- minimizing each error above and $\boldsymbol{e}_{\mathrm{OFTC}} := (i_{\mathrm{s,ref}}^{d} - \widehat{i}_{\mathrm{s,ref}}^{d}, i_{\mathrm{s,ref}}^{q} - \widehat{i}_{\mathrm{s,ref}}^{q}, i_{\mathrm{e,ref}} - \widehat{i}_{\mathrm{e,ref}})^\top$,
- minimizing the number N_{param} of parameters (storage equivalent) and
- minimizing the number N_{flop} of FLOPs (execution time equivalent).

Example applications: ANN-based control

Optimal feedforward torque control (OFTC) of electrical drives (see, e.g., [24, 173, 174]): ANN-based OFTC of EESMs

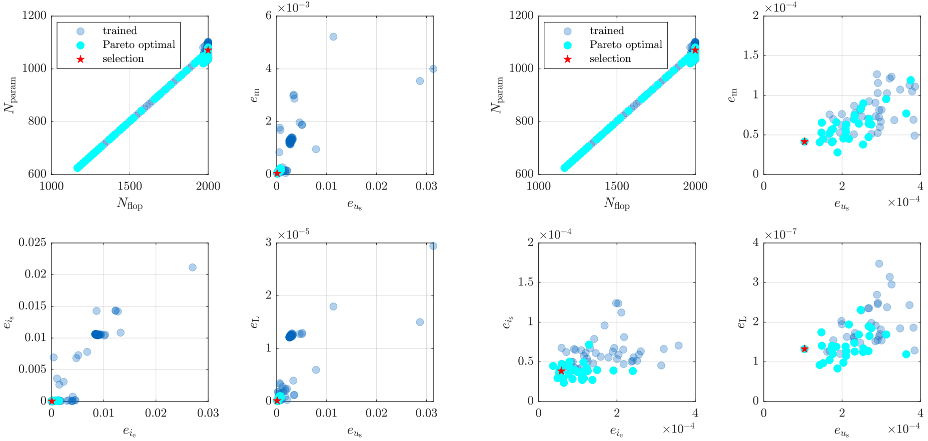

$\Longrightarrow$ Pareto optimal design (★) of the ANN with three hidden layers with $n_1 = 39$, $n_2 = 4$ and $n_3 = 83$ neurons per hidden layer as trade-off between the OFTC criteria (i.e., $N_{\mathrm{flop}} = 2000$, $N_{\mathrm{param}} = 1071$, $e_{u_s} = 10.4 \cdot 10^{-5}$, $e_{i_s} = 3.8 \cdot 10^{-5}$, $e_{i_e} = 5.8 \cdot 10^{-5}$, $e_{\mathrm{m}} = 4.1 \cdot 10^{-5}$, $e_{\mathrm{L}} = 0.1 \cdot 10^{-7}$)

Example applications: ANN-based control

Optimal feedforward torque control (OFTC) of electrical drives (see, e.g., [24, 173, 174]): ANN-based OFTC of EESMs

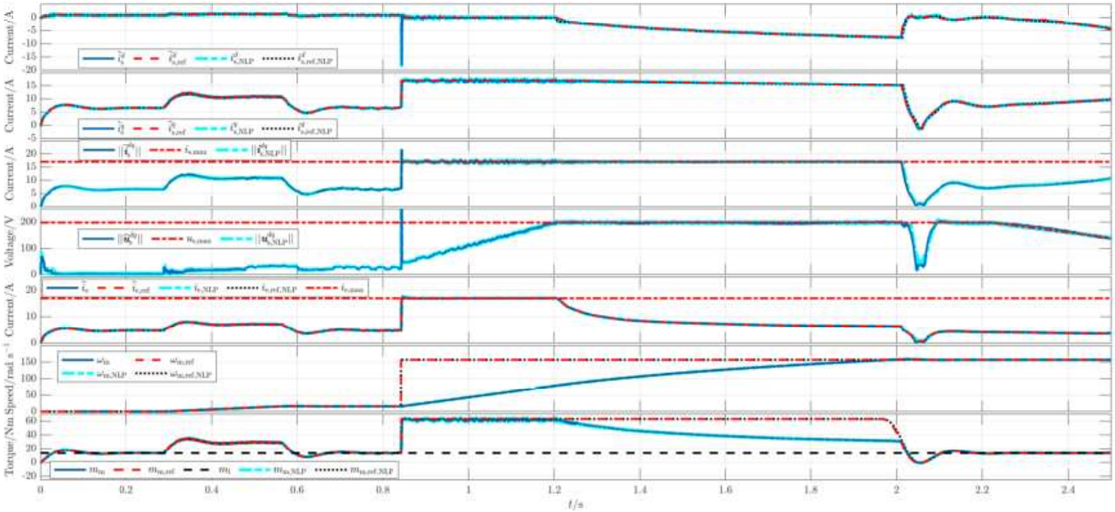

Figure: Implementation results for the proposed ANN-based OFTC for a real, nonlinear EESM.

Outline

4 Conclusion

Conclusion

To take home

- **Artificial neural networks** are
  - a (very) **powerful tool** (but imho not the solution to everything in contrast to many statements)
  - (or might be) **beneficial** (in particular with respect to memory usage or computational time)
  - **applicable** in electrical drives (e.g., for OFTC, self-commissioning, control)
  - **to be handled with care** (optimization not trivial, recall non-convergence, local minimum, etc.)
- **Artificial neural networks** require
  - **experience** (data set generation, selection of topology, activation functions, etc.)
  - **computational power** (in particular for meta studies)
  - **high storage capabilities** (at least during off-line training)
  - **physical understanding** (imho good models are crucial for proper (i.e., structured) ANN design)
- **Enjoy using ANNs and AI,**
  - but **always know and understand what you are doing** and **exploit engineering knowledge** for (e.g., structured) ANNs!
  - and, if engineering knowledge is not available, **use Pareto optimal ANN topologies accounting for limited resources** for real-time implementation (avoid trial-and-error approaches)!

References I

[1] Christoph M. Hackl. A physics-based model of electro-active polymer actuators as the bases for a Gopinath-style motion state observer. Bachelorthesis, Lehrstuhl für Elektrische Antriebssysteme, Technische Universität München, Germany & Department of Mechanical Engineering and Department of Electrical & Computer Engineering, University of Wisconsin-Madison, USA, 2003.

[2] Christoph Hackl, H.-Y. Tang, R.D. Lorenz, L.-S. Turng, and Dierk Schröder. A multiphysics model of planar electro-active polymer actuators. In *Conference Record of the 39th IEEE Industrial Application Society Annual Meeting*, volume 3, pages 2125–2130. Institute of Electrical and Electronics Engineers (IEEE), 2004.

[3] Christoph Hackl, H.-Y. Tang, R.D. Lorenz, L.-S. Turng, and Dierk Schröder. A multidomain model of planar electro-active polymer actuators. *IEEE Transactions on Industry Applications*, 41(5):1142–1148, sep 2005.

[4] Christoph M. Hackl and Beatrix Mair. Optimale Bahnzugregelung am Beispiel einer Papierstreichanlage. In *Konferenzband des 9. Bahnlaufseminar*, TU Chemnitz, Deutschland, 2007.

[5] Christoph M. Hackl and Beatrix Mair. Optimierung der Bahnspannungsregelung durch dezentrale Regelsysteme auf der Basis von moderner Mikroelektronik und intelligenter Software zur Steigerung der Produktionssicherheit und der Produktivität von Papierstreichanlagen. Abschlussbericht zum Forschungsvorhaben AiF/IGF 14140N, Arbeitsgemeinschaft industrieller Forschungsvereinigungen "Otto von Guerick" (AiF), 2007.

[6] Beatrix Mair and Christoph M. Hackl. Optimierung der Bahnspannungsregelung durch dezentrale Regelsysteme auf der Basis von moderner Mikroelektronik und intelligenter Software zur Steigerung der Produktionssicherheit und der Produktivität von Papierstreichanlagen. PTS Forschungsbericht, The Paper Technology Specialists, Hessstr. 134, 80797 München, Germany, 2007.

[7] Christoph M. Hackl and Beatrix Mair. Besser Bahnen ziehen – Optimale Bahnzugregelung mit dSPACE-Prototyping-System. *dSPACE Magazine*, 2:40–45, 2008.

[8] Christoph M. Hackl and Beatrix Mair. Smoothing the tension - optimal web tension control with a dSPACE prototyping system. *dSPACE Magazine*, 2:40–45, 2008.

[9] Christian Endisch, Christoph Hackl, and Dierk Schröder. Optimal brain surgeon for general dynamic neural networks. In José Neves, Manuel Filipe Santos, and José Manuel Machado, editors, *Progress in Artificial Intelligence*, volume 4974/2007 of *Lecture Notes in Artificial Intelligence*, pages 15–28. Springer-Verlag, Berlin, 2007.

References II

[10] Christian Endisch, Christoph Hackl, and Dierk Schröder. System identification with general dynamic neural networks and network pruning. *International Journal of Computational Intelligence*, 4(3):187–195, 2007.

[11] Christian. Endisch, Peter Stolze, Peter Endisch, Christoph M.. Hackl, and Ralph M. Kennel. Levenberg-Marquardt-based OBS algorithm using adaptive pruning interval for system identification with dynamic neural networks. In *Proceedings of the IEEE International Conference on Systems, Man and Cybernetics*, pages 3402–3408, San Antonio, TX, USA, oct 2009. Institute of Electrical and Electronics Engineers (IEEE).

[12] C. Endisch, P. Stolze, C. Hackl, and D. Schröder. Comments on “Backpropagation algorithms for a broad class of dynamic networks”. *IEEE Transactions on Neural Networks*, 20(3):540–541, mar 2009.

[13] Mohamed Abdelrahem, Christoph Hackl, and Ralph Kennel. Application of extended kalman filter to parameter estimation of doubly-fed induction generators in variable-speed wind turbine systems. In *2015 International Conference on Clean Electrical Power (ICCEP)*. IEEE.

[14] Christoph M. Hackl. Speed funnel control with disturbance observer for wind turbine systems with elastic shaft. In *Proceedings of the 54th IEEE Conference on Decision and Control (CDC 2015)*, pages 2005–2012, Osaka, Japan, 2015.

[15] Simon Krüner and Christoph M. Hackl. Experimental identification of the optimal current vectors for a permanent-magnet synchronous machine in wave energy converters. *Energies*, 12(862), 2019.

[16] Christoph M. Hackl and Markus Landerer. A unified method for online detection of phase variables and symmetrical components of unbalanced three-phase systems with harmonic distortion. *Energies*, 12(17), 2019.

[17] Mohamed Abdelrahem, Ralph Kennel, Christoph Hackl, Mehmet Dal, and José Rodríguez. Efficient finite-position-set mras observer for encoder-less control of dfigs. In *2019 IEEE International Symposium on Predictive Control of Electrical Drives and Power Electronics (PRECEDE)*, pages 1–6, May 2019.

[18] Christoph M. Hackl and Markus Landerer. A unified method for generic signal parameter estimation of arbitrarily distorted single-phase grids with dc-offset. *IEEE Open Journal of the Industrial Electronics Society*, 1:235–246, 2020.

References III

[19] T. Kreppel, F. Rojas, C. M. Hackl, O. Kalmbach, M. Díaz, and G. Gatica. Extended Model of Chopper Cells for Open Circuit Fault Detection in Modular Multilevel Cascade Converters using Sliding Mode Observers. In *2020 IEEE 11th International Symposium on Power Electronics for Distributed Generation Systems (PEDG)*, pages 487–493, 2020. ISSN: 2329-5767.

[20] Mostafa Ahmed, Mohamed Abdelrahem, Ralph Kennel, and Christoph M. Hackl. A robust maximum power point tracking based model predictive control and extended kalman filter for pv systems. In *2020 International Symposium on Power Electronics, Electrical Drives, Automation and Motion (SPEEDAM)*, pages 514–519, 2020.

[21] Mostafa Ahmed, Mohamed Abdelrahem, Ralph Kennel, and Christoph M. Hackl. Maximum power point tracking based model predictive control and extended kalman filter using single voltage sensor for pv systems. In *2020 IEEE 29th International Symposium on Industrial Electronics (ISIE)*, pages 1039–1044, 2020.

[22] Christoph M. Hackl and Markus Landerer. Modified second-order generalized integrators with modified frequency locked loop for fast harmonics estimation of distorted single-phase signals. *IEEE Transactions on Power Electronics*, 2020.

[23] Julian Kullick and Christoph M Hackl. Nonlinear modeling, identification and optimal feedforward torque control of induction machines using steady-state machine maps. *IEEE Transactions on Industrial Electronics*, pages 1–1, 2022.

[24] Max A. Buettner, Niklas Monzen, and Christoph M. Hackl. Artificial neural network based optimal feedforward torque control of interior permanent magnet synchronous machines: A feasibility study and comparison with the state-of-the-art. *Energies*, 15(5):1838, 2022.

[25] Shih-Wei Su, Christoph M. Hackl, and Ralph Kennel. Analytical prototype functions for flux linkage approximation in synchronous machines. *IEEE Open Journal of the Industrial Electronics Society*, 3:265–282, 2022.

[26] Shih-Wei Su, Hannes Börngen, Christoph M. Hackl, and Ralph Kennel. Nonlinear current control of reluctance synchronous machines with analytical flux linkage prototype functions. *IEEE Open Journal of the Industrial Electronics Society*, pages 1–12, 2022.

[27] Christoph M. Hackl. *Contributions to High-gain Adaptive Control in Mechatronics*. PhD thesis, Lehrstuhl für Elektrische Antriebssysteme und Leistungselektronik, Technische Universität München (TUM), Germany, 2012.

References IV

[28] Christoph M. Hackl. Dynamische Reibungsmodellierung: Das Lund-Grenoble (LuGre) Reibmodell. In Dierk Schröder, editor, *Elektrische Antriebe – Regelung von Antriebssystemen*, chapter 25, pages 1615–1657. Springer-Verlag, 2015.

[29] Christoph M. Hackl. Dynamische Reibungsmodellierung: Das Lund-Grenoble (LuGre) Reibmodell. In Dierk Schröder, editor, *Elektrische Antriebe – Regelung von Antriebssystemen*, chapter 9.4, pages 1315–1357. Springer-Verlag, 2020.

[30] Hans Schuster, Christoph Michael Hackl, Christian Westermaier, and Dierk Schröder. Funnel-control for electrical drives with uncertain parameters. In *Proceedings of the 7th International Power Engineering Conference*, Singapore, 2005.

[31] Christoph M. Hackl and Dierk Schröder. Extension of high-gain controllable systems for improved accuracy. In *Proceedings of the 2006 IEEE International Conference on Control Applications (CCA 2006)*, pages 2231–2236, Munich, Germany, oct 2006. Institute of Electrical and Electronics Engineers (IEEE).

[32] Christoph Michael Hackl and Dierk Schröder. Funnel-control for nonlinear multi-mass flexible systems. In *Proceedings of the 32nd Annual Conference on IEEE Industrial Electronics*, pages 4707–4712, Paris, France, 2006.

[33] Christoph M. Hackl, Hans Schuster, Christian Westermaier, and Dierk Schröder. Funnel-control with integrating prefilter for nonlinear, time-varying two-mass flexible servo systems. In *Proceedings of the 9th International Workshop on Advanced Motion Control*, pages 456–461, Istanbul, Turkey, 2006. Institute of Electrical and Electronics Engineers (IEEE).

[34] Christoph M. Hackl, Yang Ji, and Dierk Schröder. Enhanced funnel-control with improved performance. In *Proceedings of the 15th Mediterranean Conference on Control and Automation*, pages Paper T01–016, Athens, Greece, jun 2007. Institute of Electrical and Electronics Engineers (IEEE).

[35] Christoph M. Hackl, Yang Ji, and Dierk Schröder. Funnel-control with constrained control input compensation. In *Proceedings of the 9th IASTED International Conference CONTROL AND APPLICATIONS*, pages 147–152, Montreal, Quebec, Canada, 2007.

[36] Christoph M. Hackl, Yang Ji, and Dierk Schröder. Nonidentifier-based adaptive control with saturated control input compensation. In *Proceedings of the 15th Mediterranean Conference on Control and Automation*, pages Paper T01–15, Athens, Greece, jun 2007. Institute of Electrical and Electronics Engineers (IEEE).

References V

[37] Christoph M. Hackl and Dierk Schröder. Funnel-control with online foresight. In *Proceedings of the 26th IASTED International Conference MODELLING, IDENTIFICATION AND CONTROL*, pages 171–176, Innsbruck, Austria, 2007.

[38] Christoph M. Hackl and Dierk Schröder. Non-identifier based adaptive control in robotics: An introduction. *International Journal of Factory Automation, Robotics and Soft Computing*, 4:90–99, 2008.

[39] Christoph M. Hackl, Christian Endisch, and Dierk Schröder. Specially designed funnel-control in mechatronics. In *Proceedings of the 5th International Conference on Computational Intelligence, Robotics and Autonomous Systems*, pages 59–64, 2008.

[40] Christoph M. Hackl, Christian Endisch, and Dierk Schröder. Contributions to non-identifier based adaptive control in mechatronics. *Robotics and Autonomous Systems, Elsevier*, 57(10):996–1005, 2009.

[41] Christoph M. Hackl. Funnel Control: Implementierung, Erweiterung und Anwendung. In Dierk Schröder, editor, *Intelligente Verfahren: Systemidentifikation und Regelung nichtlinearer Systeme*, pages 697–760. Springer-Verlag, Berlin, 2010.

[42] Christoph M. Hackl and Stephan Trenn. The bang-bang funnel controller: An experimental verification. *PAMM*, 12(1):735–736, dec 2012.

[43] Christoph M. Hackl, Norman Hopfe, Achim Ilchmann, Markus Mueller, and Stephan Trenn. Funnel control for systems with relative degree two. *SIAM Journal on Control and Optimization*, 51(2):965–995, jan 2013.

[44] Christoph M. Hackl. Funnel control for wind turbine systems. In *Proceedings of the 2014 IEEE International Conference on Control Applications (CCA 2014)*, pages 1377–1382, Antibes, France, oct 2014. Institute of Electrical and Electronics Engineers (IEEE).

[45] Christoph M. Hackl. Current PI-funnel control with anti-windup for synchronous machines. In *Proceedings of the 54th IEEE Conference on Decision and Control (CDC 2015)*, pages 1997–2004, Osaka, Japan, dec 2015. Institute of Electrical and Electronics Engineers (IEEE).

[46] Christoph M. Hackl. *Non-identifier based adaptive control in mechatronics: Theory and Application*. Number 466 in Lecture Notes in Control and Information Sciences. Springer International Publishing, Berlin, 2017.

[47] Christoph M. Hackl, Christian Endisch, and Dierk Schröder. Applicability of funnel-control in robotics. In *Proceedings of the 5th International Conference on Computational Intelligence, Robotics and Autonomous Systems*, pages 65–70, Linz, Austria, 2008.

References VI

[48] Christoph M. Hackl, Christian Endisch, and Dierk Schröder. Funnel-control in robotics: An introduction. In *Proceedings of the 16th Mediterranean Conference on Control and Automation*, pages 913–919, Ajaccio, France, jun 2008. Institute of Electrical and Electronics Engineers (IEEE).

[49] Christoph M. Hackl and Dierk Schröder. Non-identifier based adaptive control in robotics: An introduction. In Salvatore Pennacchio, editor, *Recent adavances in Control Systems, Robotics and Automation*, volume 1. INTERNATIONALSAR International Society for Advanced Research, Palermo, Italy, third edition, 2009.

[50] Christoph M. Hackl. High-gain adaptive position control. *International Journal of Control*, 84(10):1695–1716, oct 2011.

[51] Christoph M. Hackl, Andreas G. Hofmann, Rik W. De Doncker, and Ralph M. Kennel. Funnel control for speed & position control of electrical drives: A survey. In *Proceedings of the 19th Mediterranean Conference on Control & Automation (MED)*, pages 181–188, Corfu Island, Greece, jun 2011. Institute of Electrical and Electronics Engineers (IEEE).

[52] Christoph M. Hackl, Andreas G. Hofmann, and Ralph M. Kennel. Funnel control in mechatronics: An overview. In *Proceedings of the 50th IEEE Conference on Decision and Control (CDC) and European Control Conference (ECC)*, pages 8000–8007, Orlando, FL, USA, dec 2011. Institute of Electrical and Electronics Engineers (IEEE).

[53] Christoph M. Hackl. 'Funnel control' zur Positionsregelung von starren Drehgelenkrobotern mit grob bekannter Trägheitsmatrix. In *Tagungsband des GMA-Fachausschuss 1.40*, pages 302–310, Anif, Austria, 2012.

[54] Christoph M. Hackl and Ralph M. Kennel. Position funnel control for rigid revolute joint robotic manipulators with known inertia matrix. In *Proceedings of the 20th Mediterranean Conference on Control and Automation*, pages 615–620, Barcelona, Spain, jul 2012. Institute of Electrical and Electronics Engineers (IEEE).

[55] Christoph M. Hackl and Ralph M. Kennel. Position funnel control with linear internal model. In *Proceedings of 2012 IEEE International Conference on Control Applications (CCA 2012)*, pages 1334–1339, Dubrovnik, Croatia, oct 2012. Institute of Electrical and Electronics Engineers (IEEE).

[56] Timm Faulwasser and Christoph M. Hackl. Path-following funnel control for rigid-link revolute-joint robotic systems. In *Proceedings of the 21st International Symposium on Mathematical Theory of Networks and Systems*, pages 1044–1051, Groningen, Netherlands, 2014.

References VII

[57] Julian Kullick and Christoph Hackl. Dynamic Modeling and Simulation of Deep Geothermal Electric Submersible Pumping Systems. *Energies*, 10(10):1659, October 2017.

[58] Florian Bauer, Christoph M. Hackl, Keyue Ma Smedley, and Ralph M. Kennel. Multicopter with series connected propeller drives. *IEEE Transactions on Control Systems Technology*, pages 1–12, 2017.

[59] Christoph M. Hackl, Florian Larcher, Alexander Dötlinger, and Ralph. M. Kennel. Is multiple-objective model-predictive control "optimal"? In *Proceedings of the 2013 IEEE International Symposium on Predictive Control of Electrical Drives and Power Electronics (PRECEDE 2013)*, pages 1–8, Munich, Germany, oct 2013. Institute of Electrical and Electronics Engineers (IEEE).

[60] Z. Zhang, C. Hackl, F. Wang, Z. Chen, and R. Kennel. Encoderless model predictive control of back-to-back converter direct-drive permanent-magnet synchronous generator wind turbine systems. In *Proceedings of 15th European Conference on Power Electronics and Applications*, pages 1–10. Institute of Electrical and Electronics Engineers (IEEE), sep 2013.

[61] Mohamed Abdelrahem, Christoph M. Hackl, and Ralph Kennel. Sensorless control of doubly-fed induction generators in variable-speed wind turbine systems. In *Proceedings of the 5th International Conference on Clean Electrical Power (ICCEP)*, pages 423–430, Taormina, Italy, jun 2015. Institute of Electrical and Electronics Engineers (IEEE).

[62] Christian Dirscherl, Josef Fessler, Christoph Hackl, and Hanko Ipach. State-feedback control and observer design of grid-connected power inverters with LCL-filter. In *Proceedings of the 5th Colloquium of the Munich School of Engineering*, Garching, Germany, 2015.

[63] Christian Dirscherl, Josef Fessler, Christoph M. Hackl, and Hanko Ipach. State-feedback controller and observer design for grid-connected voltage source power converters with LCL-filter. In *Proceedings of the 2015 IEEE International Conference on Control Applications (CCA 2015)*, pages 215–222, Sydney, Australia, sep 2015. Institute of Electrical and Electronics Engineers (IEEE).

[64] Christian Dirscherl, Christoph Hackl, and Korbinian Schechner. Explicit model predictive control with disturbance observer for grid-connected voltage source power converters. In *Proceedings of the 2015 IEEE International Conference on Industrial Technology (ICIT 2015)*, pages 999–1006. Institute of Electrical and Electronics Engineers (IEEE), mar 2015.

References VIII

[65] Christian Dirscherl, Christoph M. Hackl, and Korbinian Schechner. Pole-placement based nonlinear state-feedback control of the DC-link voltage in grid-connected voltage source power converters: A preliminary study. In *Proceedings of the 2015 IEEE International Conference on Control Applications (CCA 2015)*, pages 207–214, Sydney, Australia, sep 2015. Institute of Electrical and Electronics Engineers (IEEE).

[66] Christoph M. Hackl. MPC with analytical solution and integral error feedback for LTI MIMO systems and its application to current control of grid-connected power converters with LCL-filter. In *Proceedings of the 2015 IEEE International Symposium on Predictive Control of Electrical Drives and Power Electronics (PRECEDE 2015)*, pages 61–66, Valparaiso, Chile, oct 2015. Institute of Electrical and Electronics Engineers (IEEE).

[67] Zhenbin Zhang, Hue Xu, M. Xue, Z. Chen, T. Sun, Ralph Kennel, and Christoph Hackl. Predictive control with novel virtual flux estimation for back-to-back power converters. *IEEE Transactions on Industrial Electronics*, 62(5):2823–2834, may 2015.

[68] Ayman Ayad, Mohamed Hashem, Christoph Hackl, and Ralph Kennel. Proportional-resonant controller design for quasi-Z-source inverters with LC filters. In *Proceedings of the 42nd IEEE Industrial Electronics Conference (IECON 2016)*, Firenze, Italy, 2016.

[69] Christoph M. Hackl. On the equivalence of proportional-integral and proportional-resonant controllers with anti-windup. *arXiv:1610.07133*, 2016.

[70] Josh C. Mitchell, Maarten J. Kamper, and Christoph M. Hackl. Small-scale reluctance synchronous generator variable speed wind turbine system with DC transmission linked inverters. In *Proceedings of the IEEE Energy Conversion Congress & Exposition (ECCE)*, Milwaukee, WI, USA, 2016.

[71] Zhenbin Zhang, Christoph Hackl, Mohamed Abdelrahem, and Ralph Kennel. Voltage sensorless direct model predictive control of 3L-NPC back-to-back power converter PMSG wind turbine systems with fast dynamics. In *Proceedings of the Power Electronics Student Summit (PESS 2016)*, Aachen, Germany, 2016.

[72] Zhenbin Zhang, Christoph Hackl, and Ralph Kennel. Computationally efficient DMPC for three-level NPC back-to-back converters in wind turbine systems with PMSG. *IEEE Transactions on Power Electronics*, 32:8018–8034, 2017.

[73] Zhenbin Zhang, Christoph Hackl, and Ralph Kennel. FPGA based direct model predictive current control of PMSM drives with 3L-NPC power converters. In *Proceedings of the PCIM Europe 2016*, 2016.

References IX

[74] Zhenbin Zhang, Ralph Kennel, and Christoph Hackl. Computationally efficient direct model predictive control for three-level NPC back-to-back converter PMSG wind turbine systems. In *Proceedings of the 2016 International Symposium on Power Electronics, Electrical Drives, Automation and Motion (SPEEDAM 2016)*, pages 1045–1050, Anacapri, Italy, jun 2016. Institute of Electrical and Electronics Engineers (IEEE).

[75] Zhenbin Zhang, Ralph Kennel, and Christoph M. Hackl. Performance-enhanced direct multiple-vector model predictive power control for grid-tied AFEs. In *Proceedings of the 2016 IEEE 8th International Power Electronics and Motion Control Conference (IPEMC-ECCE Asia)*, pages 2904–2909, Hefei, China, may 2016. Institute of Electrical and Electronics Engineers (IEEE).

[76] Mohamed Abdelrahem, Christoph Michael Hackl, and Ralph Kennel. Finite set model predictive control with on-line parameter estimation for active frond-end converters. *Electrical Engineering*, 100(3):1497–1507, Sep 2018.

[77] M. Espinoza, R. Cardenas, J. C. Clare, D. Soto, M. Diaz, E. Espina, and C. M. Hackl. An integrated converter and machine control system for mmc-based high power drives. *IEEE Transactions on Industrial Electronics*, PP(99):1–1, 2018.

[78] Christoph M. Hackl, Urs Pecha, and Korbinian Schechner. Modeling and control of permanent-magnet synchronous generators under open-switch converter faults. *IEEE Transactions on Power Electronics*, 2018.

[79] Korbinian Schechner, Florian Bauer, and Christoph M. Hackl. Nonlinear DC-link PI control for airborne wind energy systems during pumping mode. In Roland Schmehl, editor, *Airborne Wind Energy: Advances in Technology Development and Research*. Springer Singapore, 2019.

[80] M. Diaz, R. Cardenas, M. Espinoza, C. M. Hackl, F. Rojas, J. C. Clare, and P. Wheeler. Vector control of a modular multilevel matrix converter operating in the full output-frequency range. *IEEE Transactions on Industrial Electronics*, 66(7):5102–5114, July 2019.

[81] Michael Saegmueller, Christoph Hackl, Rolf Witzmann, and Rene Richter. Analytic solutions for minimum conduction loss modulation of dual active bridge converters including frequency variation. In *IECON 2020 The 46th Annual Conference of the IEEE Industrial Electronics Society*. IEEE, oct 2020.

[82] O. Kalmbach, C. M. Hackl, and F. Rojas. A Generic Switching State-Space Model for Modular Multilevel Cascade Converters. In *2020 IEEE 11th International Symposium on Power Electronics for Distributed Generation Systems (PEDG)*, pages 447–454, 2020.

References X

[83] Oliver Kalmbach, Christian Dirscherl, and Christoph M. Hackl. Discrete-Time DC-Link Voltage and Current Control of a Grid-Connected Inverter with LCL-Filter and Very Small DC-Link Capacitance. *Energies*, 13(21):5613, 2020.

[84] Mostafa Ahmed, Mohamed Abdelrahem, Ralph Kennel, and Christoph M. Hackl. An enhanced maximum power point tracking based finite-control-set model predictive control for pv systems. In *2020 11th Power Electronics, Drive Systems, and Technologies Conference (PEDSTC)*, pages 1–6, 2020.

[85] Christoph Hackl, Christian Dirscherl, and Korbinian Schechner. Modellierung und Regelung von Windkraftanlagen (see https://arxiv.org/abs/1703.08661 for the english translation). In Dierk Schröder, editor, *Elektrische Antriebe – Regelung von Antriebssystemen*, chapter 10.3, pages 1504–1585. Springer-Verlag, 2020.

[86] Michael Saegmueller, Christoph Hackl, Rolf Witzmann, and René Richter. Analytic solutions for full operating range single-side zvs modulation of dual active bridge converters. In *Proceedings of the IEEE International Symposium on Industrial Electronics (ISIE) 2021*. IEEE, 2021.

[87] Christoph Hackl, Simon Krüner, and Zhao Song. 3d-modulation and pi state-feedback control for voltage source inverters with split dc-link. In *Proceedings of the IEEE International Symposium on Industrial Electronics (ISIE) 2021*. IEEE, 2021.

[88] Ibrahim Harbi, Mostafa Ahmed, Christoph M. Hackl, Ralph Kennel, and Mohamed Abdelrahem. A nine-level split-capacitor active-neutral-point-clamped inverter and its optimal modulation technique. *IEEE Transactions on Power Electronics*, 37(7):8045–8064, 2022.

[89] Christoph M. Hackl, Christian Endisch, and Dierk Schröder. Error reference control of nonlinear two-mass flexible servo systems. In *Proceedings of the 16th Mediterranean Conference on Control and Automation*, pages 1047–1053, Ajaccio, France, jun 2008. Institute of Electrical and Electronics Engineers (IEEE).

[90] Peter Landsmann, Christoph M. Hackl, and Ralph M. Kennel. Eliminating all machine parameters in encodersless predictive torque control without signal injection. In *Proceedings of the 2011 IEEE International Electric Machines and Drives Conference*, pages 1259–1264. Institute of Electrical and Electronics Engineers (IEEE), may 2011.

References XI

[91] Christoph M. Hackl. Funnel control with disturbance observer for two-mass systems. In *Proceedings of the 52nd IEEE Conference on Decision and Control (CDC)*, pages 6244–6249, Florence, Italy, dec 2013. Institute of Electrical and Electronics Engineers (IEEE).

[92] Christoph M. Hackl. PI-funnel control with Anti-windup and its application for speed control of electrical drives. In *Proceedings of the 52nd IEEE Conference on Decision and Control (CDC)*, pages 6250–6255, Florence, Italy, dec 2013. Institute of Electrical and Electronics Engineers (IEEE).

[93] Christian Dirscherl, Christoph M. Hackl, and Korbinian Schechner. Modeling and control of wind turbine systems with permanent-magnet synchronous generators (PMSG) and doubly fed induction generators (DFIG). In *Proceedings of the 4th Colloquium of the Munich School of Engineering*, Garching, Germany, 2014.

[94] Christoph M. Hackl. Klein-Windkraftanlagen mit effizienter und kostengünstiger Generatortopologie für Micro-Grids: Eine Voruntersuchung. In *Poster auf der Jahresversammlung des Bundes der Freunde der Technischen Universität München e.V.*, Munich, Germany, 2014.

[95] Christoph Hackl and Korbinian Schechner. Non-ideal torque control in wind turbine systems: Causes and impacts. In *Proceedings of the 5th Colloquium of the Munich School of Engineering*, Garching, Germany, 2015.

[96] Christoph M. Hackl, Maarten J. Kamper, Julian Kullick, and Joshua Mitchell. Nonlinear PI current control of reluctance synchronous machines. 2015.

[97] Christoph M. Hackl and Korbinian Schechner. Non-ideal torque control in wind turbine systems: Causes and impacts. In *Proceedings of the 5^{th} MSE-Kolloquium on "Innovations for Energy Systems, Mobility, Buildings and Materials"*, Munich, Germany, 2015.

[98] Mohamed Abdelrahem, Christoph M. Hackl, and Ralph Kennel. Encoderless model predictive control of doubly-fed induction generators in variable-speed wind turbine systems. In *Proceedings of the 6th edition of the conference "The Science of Making Torque from Wind" (TORQUE 2016)*, Open access Journal of Physics: Conference Series 753 (2016) 112005, Munich, Germany, 2016.

References XII

[99] Hisham Eldeeb, Christoph M. Hackl, Lorenz Horlbeck, and Julian Kullick. On the optimal feedforward torque control problem of anisotropic synchronous machines: Quadrics, quartics and analytical solutions. 2016.

[100] Hisham Eldeeb, Christoph M. Hackl, and Julian Kullick. Efficient operation of anisotropic synchronous machines for wind energy systems. In *Proceedings of the 6th edition of the conference "The Science of Making Torque from Wind" (TORQUE 2016)*, Open access Journal of Physics: Conference Series 753 (2016) 112005, Munich, Germany, 2016.

[101] Christoph M. Hackl, Maarten J. Kamper, Julian Kullick, and Joshua Mitchell. Current control of reluctance synchronous machines with online adjustment of the controller parameters. In *Proceedings of the 2016 IEEE International Symposium on Industrial Electronics (ISIE 2016)*, pages 153–160. Institute of Electrical and Electronics Engineers (IEEE).

[102] Lorenz Horlbeck and Christoph M. Hackl. Analytical solution for the MTPV hyperbola including the stator resistance. In *Proceedings of the IEEE International Conference on Industrial Technology (ICIT 2016)*, pages 1060–1067, Taipei, Taiwan, mar 2016. Institute of Electrical and Electronics Engineers (IEEE).

[103] Zhenbin Zhang, Ralph Kennel, and Christoph M. Hackl. Two direct torque and power control methods for back-to-back power converter PMSG wind turbine systems. In *Proceedings of the 2016 IEEE 8th International Power Electronics and Motion Control Conference (IPEMC-ECCE Asia)*, pages 1515–1520, Hefei, China, may 2016. Institute of Electrical and Electronics Engineers (IEEE).

[104] Mohamed. Abdelrahem, Christoph Hackl, and Ralph Kennel. Finite Position Set-Phase Locked Loop for Sensorless Control of Direct-Driven Permanent-Magnet Synchronous Generators. *IEEE Transactions on Power Electronics*, PP(99):1–1, 2017.

[105] Hisham Eldeeb, Christoph M. Hackl, Lorenz Horlbeck, and Julian Kullick. A unified theory for optimal feedforward torque control of anisotropic synchronous machines. *International Journal of Control*, 2017.

[106] Hisham Eldeeb, Christoph M. Hackl, Lorenz Horlbeck, and Julian Kullick. Analytical solutions for the optimal reference currents for MTPC/MTPA, MTPV and MTPF control of anisotropic synchronous machines. In *Proceedings of the IEEE International Electric Machines & Drives Conference (IEMDC 2017)*, pages 1–6, Miami, FL, USA, 2017.

[107] Mohamed Abdelrahem, Christoph Michael Hackl, and Ralph Kennel. Implementation and experimental investigation of a sensorless field-oriented control scheme for permanent-magnet synchronous generators. *Electrical Engineering*, may 2017.

References XIII

[108] A. D. Birda, J. Reuss, and C. Hackl. Synchronous optimal pulse-width modulation with differently modulated waveform symmetry properties for feeding synchronous motor with high magnetic anisotropy. In *2017 19th European Conference on Power Electronics and Applications (EPE'17 ECCE Europe)*, pages P.1–P.10, Sept 2017.

[109] H. Eldeeb, C. Hackl, M. Abdelrahem, and A. S. Abdel-Khalik. A unified SVPWM realization for minimizing circulating currents of dual three phase machines. In *2017 IEEE 12th International Conference on Power Electronics and Drive Systems (PEDS)*, pages 925–931, Dec 2017.

[110] Mauricio Espinoza, Matias Díaz, Enrique Espina, Christoph M. Hackl, and Roberto Cardénas. Control strategies for modular multilevel converters driving cage machines. In *Proceedings of the 3rd IEEE Southern Power Electronics Conference (SPEC 2017)*, pages 1–6, Dec 2017.

[111] Mohamed Abdelrahem, Christoph M. Hackl, Zhenbin Zhang, and Ralph Kennel. Robust predictive control for direct-driven surface-mounted permanent-magnet synchronous generators without mechanical sensors. *IEEE Transactions on Energy Conversion*, 33(1):179–189, 2018.

[112] Korbinian Schechner and Christoph M. Hackl. Scaling of the drive train dynamics of large-scale wind turbine systems for real-time emulation in small-scale laboratory setups. *IEEE Transactions on Industrial Electronics*, 66(9):6779–6788, 2018.

[113] H. Eldeeb, A. S. Abdel-Khalik, and C. Hackl. Dynamic modelling of dual three-phase IPMSM drives with different neutral configurations. *IEEE Transactions on Industrial Electronics*, PP(99):1–1, 2018.

[114] H. Eldeeb, M. Abdelrahem, C. Hackl, and A. S. Abdel-Khalik. Enhanced electromechanical modeling of asymmetrical dual three-phase IPMSM drives. In *2018 IEEE 27th International Symposium on Industrial Electronics (ISIE)*, pages 126–132, June 2018.

[115] H. Eldeeb, A. S. Abdel-Khalik, and C. Hackl. Post-fault full torque-speed exploitation of dual three-phase IPMSM drives. *IEEE Transactions on Industrial Electronics*, 2018.

[116] Hisham Magdy Eldeeb, Ayman Samy Abdel-Khalik, Julian Kullick, and Christoph M. Hackl. Pre and post-fault current control of dual three-phase reluctance synchronous drives. *IEEE Transactions on Industrial Electronics*, pages 1–1, 2019.

References XIV

[117] Athina Birda, Jörg Reuss, and Christoph M. Hackl. Simple fundamental current estimation and smooth transition between synchronous optimal pwm and asynchronous svm. *IEEE Transactions on Industrial Electronics*, pages 1–1, 2019.

[118] Xiaonan Gao, Mohamed Abdelrahem, Christoph M. Hackl, Zhenbin Zhang, and Ralph Kennel. Direct predictive speed control with a sliding manifold term for pmsm drives. *IEEE Journal of Emerging and Selected Topics in Power Electronics*, pages 1–1, 2019.

[119] Mohamed Abdelrahem, Christoph Michael Hackl, Ralph Kennel, and José Rodríguez. Efficient direct-model predictive control with discrete-time integral action for pmsgs. *IEEE Transactions on Energy Conversion*, 34(2):1063–1072, 2019.

[120] Mohamed Abdelrahem, Christoph Hackl, Ralph Kennel, and Jose Rodriguez. Sensorless predictive speed control of permanent-magnet synchronous generators in wind turbine applications. In *PCIM Europe 2019; International Exhibition and Conference for Power Electronics, Intelligent Motion, Renewable Energy and Energy Management*, pages 1–8, May 2019.

[121] Shih-Wei Su, Ralph Kennel, and Christoph M. Hackl. Analytical flux linkage approximation prototypes for reluctance synchronous machines. In *2020 International Symposium on Power Electronics, Electrical Drives, Automation and Motion (SPEEDAM)*. IEEE, jun 2020.

[122] Mohamed Abdelrahem, Christoph M. Hackl, José Rodríguez, and Ralph Kennel. Model reference adaptive system with finite-set for encoderless control of PMSGs in micro-grid systems. *Energies*, 13(18):4844, sep 2020.

[123] Christoph Hackl, Julian Kullick, and Niklas Monzen. Optimale Betriebsführung für nichtlineare Synchronmaschinen. In Joachim Böcker and Gerd Griepentrog, editors, *Elektrische Antriebe – Regelung von Antriebssystemen*. Springer-Verlag, 2020.

[124] Antonin Glac, Vaclav Smidl, Zdenek Peroutka, and Christoph M. Hackl. Comparison of IPMSM parameter estimation methods for motor efficiency. In *IECON 2020 The 46th Annual Conference of the IEEE Industrial Electronics Society*. IEEE, oct 2020.

[125] Christoph Hackl, Julian Kullick, and Peter Landsmann. Nichtlineare Stromregelverfahren für Reluktanz-Synchronmaschinen. In Joachim Böcker and Gerd Griepentrog, editors, *Elektrische Antriebe – Regelung von Antriebssystemen*. Springer-Verlag, 2020.

[126] Ahmed Farhan, Mohamed Abdelrahem, Christoph M. Hackl, Ralph Kennel, Adel Shaltout, and Amr Saleh. Advanced strategy of speed predictive control for nonlinear synchronous reluctance motors. *Machines*, 8(3):44, aug 2020.

References XV

[127] Mohamed Abdelrahem, Christoph Hackl, Ralph Kennel, and Jose Rodriguez. Low sensitivity predictive control for doubly-fed induction generators based wind turbine applications. *Sustainability*, 13(16):9150.

[128] Athina Birda, Joerg Reuss, and Christoph M. Hackl. Synchronous optimal pulsewidth modulation for synchronous machines with highly operating point dependent magnetic anisotropy. *IEEE Transactions on Industrial Electronics*, 68(5):3760–3769, may 2021.

[129] Athina Birda, Christoph Grabher, Joerg Reuss, and Christoph M. Hackl. Dc-link capacitor and inverter current ripples in anisotropic synchronous motor drives produced by synchronous optimal pwm. *IEEE Transactions on Industrial Electronics*, jan 2021.

[130] Andrea Zanelli, Julian Kullick, Hisham Eldeeb, Gianluca Frison, Christoph Hackl, and Moritz Diehl. Continuous control set nonlinear model predictive control of reluctance synchronous machines. *IEEE Transactions on Control Systems Technology*, pages 1–12, 2021.

[131] C. M. Hackl, J. Kullick, and N. Monzen. Generic loss minimization for nonlinear synchronous machines by analytical computation of optimal reference currents considering copper and iron losses. In *2021 IEEE International Conference on Industrial Technology (ICIT)*. IEEE, mar 2021.

[132] Mohamed Abdelrahem, Christoph M. Hackl, Ralph Kennel, and Jose Rodriguez. Computationally efficient finite-position-set-phase-locked loop for sensorless control of PMSGs in wind turbine applications. *IEEE Transactions on Power Electronics*, 36(3):3007–3016, mar 2021.

[133] Antonín Glac, Václav Šmídl, Zdeněk Peroutka, and Christoph M. Hackl. Dependence of IPMSM motor efficiency on parameter estimates. *Sustainability*, 13(16):9299.

[134] Haotian Xie, Jianming Du, Dongliang Ke, Yingjie He, Fengxiang Wang, Christoph Hackl, José Rodríguez, and Ralph Kennel. Multistep model predictive control for electrical drives—a fast quadratic programming solution. *Symmetry*, 14(3):626.

[135] Issa Hammoud, Sebastian Hentzelt, Ke Xu, Thimo Oehlschlaegel, Mohamed Abdelrahem, Christoph M. Hackl, and Ralph Kennel. On continuous set model predictive control of permanent magnet synchronous machines. *IEEE Transactions on Power Electronics*, pages 1–1, 2022.

References XVI

[136] Julian Kullick and Christoph M. Hackl. Speed-sensorless control of induction machines with LC filter for geothermal electric submersible pumping systems. *Machines*, 10(2):87.

[137] Yuebin Pang, Jovan Knezevic, Daniel Glose, and Christoph Hackl. Sensorless control of electrically excited synchronous machines considering magnetic saturation and flux linkage dynamics for automotive applications. *IEEE Transactions on Industrial Electronics*, pages 1–11.

[138] Simon Wiedemann and Christoph M. Hackl. Simultaneous identification of inverter and machine nonlinearities for self-commissioning of electrical synchronous machine drives. *IEEE Transactions on Energy Conversion*, pages 1–14, 2023.

[139] Johannes Rossmann, Maarten J. Kamper, and Christoph M. Hackl. Single-objective machine design with gaussian process regression and bayesian optimization (extended version). *techrxiv.org (preprint)*, May 2024.

[140] Johannes Rossmann, Maarten J. Kamper, and Christoph M. Hackl. Multi-objective machine design optimization withgaussian process regression and bayesianoptimization (extended version). *techrxiv.org (preprint)*, May.

[141] Christian Dirscherl, Christoph Hackl, and Korbinian Schechner. Modellierung und Regelung von modernen Windkraftanlagen: Eine Einführung (see https://arxiv.org/abs/1703.08661 for the english translation). In Dierk Schröder, editor, *Elektrische Antriebe – Regelung von Antriebssystemen*, chapter 24, pages 1540–1614. Springer-Verlag, 2015.

[142] Florian Bauer, Christoph M. Hackl, and Korbinian Schechner. DC-link control for airborne wind energy systems during pumping mode. In *Proceedings of the Airborne Wind Energy Conference (AWEC 2015)*, Delft, Netherlands, 2015.

[143] Mohamed Abdelrahem, Christoph M. Hackl, and Ralph Kennel. Model predictive control of permanent magnet synchronous generators in variable-speed wind turbine systems. In *Proceedings of the Power Electronics Student Summit (PESS 2016)*, Aachen, Germany, 2016.

[144] Mohamed Abdelrahem, Christoph Michael Hackl, and Ralph Kennel. Simplified model predictive current control without mechanical sensors for variable-speed wind energy conversion systems. *Electrical Engineering*, 99(1):367–377, 2016.

References XVII

[145] Mohamed Abdelrahem, Christoph M. Hackl, Zhenbin Zhang, and Ralph Kennel. Sensorless control of permanent magnet synchronous generators in variable-speed wind turbine systems. In *Proceedings of the Power Electronics Student Summit (PESS 2016)*, Aachen, Germany, 2016.

[146] Florian Bauer, Christoph M. Hackl, K. Smedley, and Ralph Kennel. Virtual-power-hardware-in-the-loop simulations in crosswind kite power with ground generation. In *Proceedings of the 2016 American Control Conference (ACC)*, pages 4071–4076, Boston, FL, USA, jul 2016. Institute of Electrical and Electronics Engineers (IEEE).

[147] Christian Dirscherl and Christoph M. Hackl. Dynamic power flow in wind turbine systems with doubly-fed induction generator. In *Proceedings of the 2016 IEEE International Energy Conference (ENERGYCON 2016)*, pages 1–6, Leuven, Beglium, apr 2016. Institute of Electrical and Electronics Engineers (IEEE).

[148] Christoph M. Hackl and Korbinian Schechner. Non-ideal feedforward torque control of wind turbines: Impacts on annual energy production & gross earnings. In *Proceedings of the 6th edition of the conference "The Science of Making Torque from Wind" (TORQUE 2016)*, volume 753 of *Open access Journal of Physics: Conference Series 753 (2016) 112005*, page 112010, Munich, Germany, sep 2016. IOP Publishing.

[149] Florian Bauer, Ralph M. Kennel, Christoph M. Hackl, Filippo Campagnolo, Michael Patt, and Roland Schmehl. Drag power kite with very high lift coefficient. *Renewable Energy*, October 2017.

[150] Christian Dirscherl and Christoph M. Hackl. Local stability analysis and controller design for speed-controlled wind turbine systems in regime ii.5. *Energies*, (5):33, 2018.

[151] Christoph M. Hackl, Pol Jané-Soneira, Martin Pfeifer, Korbinian Schechner, and Sören Hohmann. Full- and reduced-order state-space modeling of wind turbine systems with permanent magnet synchronous generator. *Energies*, (7):33, 2018.

[152] S. Hanif, K. Zhang, C. Hackl, M. Barati, H. B. Gooi, and T. Hamacher. Decomposition and equilibrium achieving distribution locational marginal prices using trust-region method. *IEEE Transactions on Smart Grid*, PP(99):1–1, 2018.

[153] Mohamed Abdelrahem, Christoph Hackl, Ahmed Farhan, and Ralph Kennel. Finite-set mras observer for encoderless control of pmsgs in wind turbine applications. In *2019 IEEE Conference on Power Electronics and Renewable Energy (CPERE)*, pages 431–436, 2019.

References XVIII

[154] Katharina Bär, Abdessamad Saidi, Christoph Hackl, and Wilfried Zörner. Combined operation of photovoltaic and biogas plants for optimal transformer loading. *Chemical Engineering Transactions*, 76:601–606.

[155] Kai Zhang, Sarmad Hanif, Christoph M. Hackl, and Thomas Hamacher. A framework for multi-regional real-time pricing in distribution grids. *IEEE Transactions on Smart Grid*, 10(6):6826–6838, Nov 2019.

[156] Florian Bauer, Christoph M. Hackl, Keyue Smedley, and Ralph Kennel. Crosswind kite power with tower. In Roland Schmehl, editor, *Airborne Wind Energy: Advances in Technology Development and Research*. Springer-Verlag, 2019.

[157] Florian Bauer, Christoph M. Hackl, Keyue Smedley, and Ralph Kennel. On multicopter-based launching and landing of lift power kites. In Roland Schmehl, editor, *Airborne Wind Energy: Advances in Technology Development and Research*. Springer-Verlag, 2019.

[158] Mohamed Abdelrahem, Christoph Hackl, and Ralph Kennel. Robust predictive control scheme for permanent-magnet synchronous generators based modern wind turbines. *Electronics*, 10(13):1596.

[159] D. Schröder and C.M. Hackl. Grundlagen der Regelungstechnik. IHK Schwaben, Mechatronik Weiterbildung, 2009.

[160] Christoph Hackl. *Bewegungssteuerung durch geregelte elektrische Antriebe (Übung)*. Lehrstuhl für Elektrische Antriebe und Leistungselektronik – Technische Universität München, 2013.

[161] Christoph M. Hackl. Regelung von regenerativen Energiesystemen (Vorlesungsskriptum und Übungsaufgaben). online, 2014. Lehrmaterialien zur Veranstaltung “Regelung von regenerativen Energiesystemen” im Wintersemester 2013/2014 an der Technischen Universität München.

[162] Christoph M. Hackl. Projektstudium Antriebstechnik: Projektbezogen Studieren – Aktives Lernen im Team. online, 2015. Kurzskriptum mit Projektbeschreibungen zur Umsetzung des Ernst-Otto Fischer Lehrpreises 2013 im Wintersemester 2014/2015 an der Technischen Universität München.

[163] Christoph Hackl, Ellen Taraba, and Anne-Marie Fleischmann. Projektbezogen Studieren – Aktives Lernen im Team: Fachliche und überfachliche Kompetenzen von Studierenden fördern. In *Tagungsband des 2. HD-MINT-Symposium Hochschuldidaktik für MINT-Fächer*, Nürnberg, Germany, 2015.

References XIX

[164] Christoph M. Hackl, Anne-Marie Fleischmann, and Ellen Taraba. Projektstudium Antriebstechnik: Projektbezogen Studieren – Aktives Lernen im Team. In *Tagungsband des 5. VDI Qualitätsdialogs Lehre - Studienerfolg verbessern*, Tagungswerk Jerusalemkirche, Berlin, Germany, 2015.

[165] Christoph Hackl, Anne-Marie Lickert, and Ellen Taraba. Projektbezogen Studieren – Aktives Lernen im Team. In *Neues Handbuch Hochschullehre*, volume 76, pages 31–44. DUZ Medienhaus, 2016.

[166] Shen Zhang. Artificial intelligence in electric machine drives: Advances and trends. *arXiv*, 2021.

[167] Shen Zhang, Oliver Wallscheid, and Mario Porrmann. Machine learning for the control and monitoring of electric machine drives: Advances and trends. 4:188–214.

[168] Felix Rojas, Cristobal Jerez, Christoph Michael Hackl, Oliver Kalmbach, Javier Pereda, and Jonathan Lillo. Faults in Modular Multilevel Cascade Converters—Part I: Reliability, Failure Mechanisms, and Fault Impact Analysis. *IEEE Open J. Ind. Electron. Soc.*, 3:628–649, Oct. 2022.

[169] Felix Rojas, Cristobal Jerez, Christoph M. Hackl, Oliver Kalmbach, Javier Pereda, and Jonathan Lillo. Faults in Modular Multilevel Cascade Converters—Part II: Fault Tolerance, Fault Detection and Diagnosis, and System Reconfiguration. *IEEE Open J. Ind. Electron. Soc.*, 3:594–614, Oct. 2022.

[170] Dierk Schröder and Martin Buss. *Intelligente Verfahren: Identifikation und Regelung nichtlinearer Systeme*. Springer-Verlag, Berlin, 2017.

[171] Charu C. Aggarwal. *Neural Networks and Deep Learning: A Textbook*. Springer International Publishing, Cham, 2018.

[172] Ingo Gühring, Mones Raslan, and Gitta Kutyniok. Expressivity of deep neural networks. *arXiv preprint arXiv:2007.04759*, 34, 2020.

[173] Niklas Monzen and Christoph M. Hackl. Artificial neural network based optimal feedforward torque control of electrically excited synchronous machines. In *2023 IEEE 32nd International Symposium on Industrial Electronics (ISIE)*. IEEE, 2023.

[174] Niklas Monzen, Florian Stroebl, Herbert Palm, and Christoph M. Hackl. Multiobjective hyperparameter optimization of artificial neural networks for optimal feedforward torque control of synchronous machines. *IEEE Open Journal of the Industrial Electronics Society*, 5:41–53, 2024.